DOI: 10.1534/genetics.110.116038

Functional Genomic Identification of Genes Required for Male Gonadal Differentiation in *Caenorhabditis elegans*

Andrea K. Kalis,* Mary B. Kroetz,† Kathleen M. Larson† and David Zarkower*,†,‡,1

**Program in Molecular, Cellular, Developmental Biology, and Genetics* †*Department of Genetics, Cell Biology, and Development and Developmental Biology Center* ‡*Masonic Cancer Center, University of Minnesota, Minneapolis, Minnesota 55455*

Manuscript received February 25, 2010
Accepted for publication March 11, 2010

ABSTRACT

The *Caenorhabditis elegans* somatic gonad develops from a four-cell primordium into a mature organ that differs dramatically between the sexes in overall morphology (two arms in hermaphrodites and one in males) and in the cell types comprising it. Gonadal development in *C. elegans* is well studied, but regulation of sexual differentiation, especially later in gonadal development, remains poorly elucidated. To identify genes involved in this process, we performed a genome-wide RNAi screen using sex-specifically expressed gonadal GFP reporters. This screen identified several phenotypic classes, including ~70 genes whose depletion feminized male gonadal cells. Among the genes required for male cell fate specification are Wnt/β-catenin pathway members, cell cycle regulators, and genes required for mitotic spindle function and cytokinesis. We find that a Wnt/β-catenin pathway independent of extracellular Wnt ligand is essential for asymmetric cell divisions and male differentiation during gonadal development in larvae. We also find that the cell cycle regulators *cdk-1* and *cyb-3* and the spindle/cytokinesis regulator *zen-4* are required for Wnt/β-catenin pathway activity in the developing gonad. After sex is determined in the gonadal primordium the global sex determination pathway is dispensable for gonadal sexual fate, suggesting that male cell fates are promoted and maintained independently of the global pathway during this period.

THE *Caenorhabditis elegans* gonad derives from a simple primordium of four cells that coalesces during embryogenesis and contains two somatic gonad precursors (SGPs), Z1 and Z4, flanking two germline precursors, Z2 and Z3 (Kimble and Hirsh 1979). The SGPs undergo very different developmental programs in each sex, involving sexually dimorphic cell lineages and migrations and sex-specific cellular differentiation. The result is a two-armed bilaterally symmetrical gonad in the adult hermaphrodite or a single-armed asymmetric gonad in the adult male. The high degree of sexual dimorphism of the mature organ and variety of cellular events that occur sex specifically during its development make the *C. elegans* gonad an outstanding model for sex-specific organogenesis.

Development of the somatic gonad occurs in two phases. The early phase defines the gonadal axes and establishes the precursors of the major gonadal cell types. This takes place during the first larval stage (L1), beginning shortly after hatching with the first division of the SGPs. In both sexes SGP division is asymmetric in terms of both the sizes and the fates of the daughter cells, and establishes the proximal/distal axis of the gonad (Hirsh *et al.* 1976; Kimble and Hirsh 1979). The global sex determination pathway establishes the future sex of the gonad around the time of hatching (Klass *et al.* 1976; Nelson *et al.* 1978), and sexual dimorphism is already apparent when the SGPs divide: the size asymmetry of the SGP daughters is much more pronounced in males than hermaphrodites. In both sexes the asymmetry of the first SGP division requires a Wnt/β-catenin pathway. Mutations compromising this pathway cause a "symmetrical sisters" phenotype in which both daughters adopt the same fate (Miskowski *et al.* 2001; Siegfried and Kimble 2002; Phillips and Kimble 2009). Sex specificity is imposed on the SGPs by the global sex determining gene *tra-1* (Hodgkin 1987) and the gonad-specific sex determining gene *fkh-6* (Chang *et al.* 2004). These genes play opposing roles in SGP sex determination, with *tra-1* feminizing and *fkh-6* masculinizing the somatic gonad, and they also act redundantly to promote mitotic proliferation of the SGP lineage (Chang *et al.* 2004). SGP sex determination is linked to cell cycle progression by cyclin D, which is required to overcome repression of *fkh-6* expression in the SGPs by E2F (Tilmann and Kimble 2005).

Supporting information is available online at http://www.genetics.org/cgi/content/full/genetics.110.116038/DC1.

[1]*Corresponding author:* Department of Genetics, Cell Biology, and Development, University of Minnesota, 321 Church St. SE, Minneapolis, MN 55455. E-mail: zarko001@umn.edu

The later phase of gonadal development involves the elongation of the gonad, together with cellular proliferation and differentiation, and lasts from L2 to adulthood. During L2 the somatic cells enlarge and leader cells (distal tip cells in the hermaphrodite, linker cell in the male) begin long-range migrations that extend the gonad. During L3, somatic gonad cell division resumes in both sexes, leading to the formation of differentiated somatic cell types by the end of L3 or beginning of L4. Gonadal morphogenesis is completed and gametogenesis begins during L4 (Kimble and Hirsh 1979).

Although SGP division and much of hermaphrodite gonadal development have been well studied (Hubbard and Greenstein 2000), sexual cell fate specification in the somatic gonad is more poorly understood, particularly after the L1 stage. Despite the importance of *fkh-6* in promoting male differentiation, it is expressed in males only during early L1 and null mutants have incomplete gonadal sex reversal. We have therefore performed a genome-wide RNAi screen to identify additional genes required after hatching for gonadal development in each sex. Among the advantages of this approach is the ability to identify gonadal regulators that also are essential for embryonic development. To our knowledge this is the first functional genomic study of gonadal sex differentiation.

The screen identified many genes whose depletion disrupts gonadogenesis in each sex and nearly 70 genes whose depletion causes gonadal feminization in males. Prominent among this latter class were components of a Wnt/β-catenin pathway, cell cycle regulators, and genes involved in mitotic spindle function and cytokinesis. We find that Wnt/β-catenin activity continues in both sexes after SGP division and is required for male cell fate commitment in the gonad. We also find that the cyclin-dependent kinase *cdk-1* and its cognate cyclin *cyb-3* as well as the mitotic spindle regulator *zen-4* are required for gonadal Wnt/β-catenin pathway activity, providing a potential new link between the cell cycle, asymmetric division, and sexual differentiation. The feminization caused by depletion of Wnt/β-catenin pathway components or *cdk-1* is independent of the global sex determination pathway, suggesting that sexual fates in the male gonad remain plastic after the primary sex determination decision.

MATERIALS AND METHODS

Strains and alleles: *C. elegans* were cultured and genetically manipulated as described (Sulston and Hodgkin 1988). All strains unless otherwise indicated carry the high incidence of male mutation *him-8* or *him-5*. The following mutations were used. LGI: *sys-1(q544)*, *pop-1(q624)*; LGII: *rrf-3(pk1426)*, *tra-2(ar221)*, *tra-2(e1095)*, *mig-14(ga62)*; LGIII: *cdk-1(ne2257)*, *tra-1(e1099)*; LGIV: *oma-1(zu405)*, *him-8(e1489)*; LGV: *him-5(e1490)*. The following integrated transgenes were used. LGI: *tnIs5[lim-7::GFP]*; LGIII: *ezIs2[fkh-6::GFP]*; LGIV: *tnIs6[lim-7::GFP]*; LGV: *qIs56[lag-2::GFP]*; LGX: *ezIs1[K09C8.2::GFP]*, *ezIs3[fkh-6::GFP]*; LG *unknown*: *syIs187[POPTOP]*, *qIs90[ceh-22::venus]* (gift of J. Kimble), *maIs229[Pmir-85::GFP]*. Extrachromosomal array: *syEx974[POPFOP]*, *tnEx91[ZK813.3::mCherry]* (gift of D. Greenstein). Dominant GFP balancer: *hT2[qIs48]* for LGI and LGIII.

The *oma-1* RNAi clone was constructed as described (Kamath and Ahringer 2003).

RNAi: RNAi screening was as described (Kamath and Ahringer 2003) with some modifications. Bacterial clones were grown overnight in LB containing 100 μg/ml ampicillin. A total of 30 μl of culture was seeded onto 12-well NGM medium containing 25 μg/ml carbenicillin and 0.2% lactose to induce dsRNA expression overnight at room temperature. For both experimental strains (*K09C8.2::GFP* and *fkh-6::GFP*) eggs were recovered from gravid hermaphrodites by hypochlorite treatment, dropped onto prepared plates, and incubated at 22° for 3 days. Controls for each round of RNAi included *fkh-6* (Chang *et al.* 2004) and empty *L4440* vector. Young adult animals were scored under fluorescence microscopy (Nikon SMZ1500) for missing, abnormal, or sex-inappropriate marker expression. All positive RNAi clones confirmed after retesting were sequenced. The secondary and tertiary screens were conducted by DIC and fluorescence microscopy (Leica DMRB) at ×400 with animals mounted on 2% agarose pads with 0.1% tetramisole. In the secondary screen animals were scored for gonadal defects including failure of gonadal elongation, adult germ cells, and proper adult gonadal morphology. Fertility was assessed by moving six adult hermaphrodites to a fresh RNAi plate for 3 days at 22° and scoring for presence of larvae, dead eggs, or no eggs. The tertiary screen scored for sex-inappropriate expression of the *lim-7::GFP* marker.

Double and triple RNAi were performed using plates seeded with equal parts of the bacterial cultures. *oma-1/2* RNAi was performed postembryonically by crossing N2 to *ezIs3* (non-Him) to produce males. This was necessary as *him* mutations appeared to suppress *oma-1/2(RNAi)* germline defects.

RNAi of *tra-2(ar221ts)* non-Him animals was performed by incubating young adult hermaphrodites at 25° for 3 days on plates seeded with dsRNA-producing bacteria.

Microscopy: Images were captured using a Zeiss Imager.Z1 microscope with AxioCam MRm camera and processed using Axio Vision Release 4.7 software.

Gene ontology: Gene ontologies (GO) were determined for each gene using the GO Term Mapper http://go.princeton.edu/cgi-bin/GOTermMapper. GO Term Mapper is based on map2slim, written by Chris Mungall (Harris *et al.* 2004). This script is part of the GO development suite: http://www.godatabase.org/dev/. This tool bins granular GO terms into high-level GO parent terms allowing comparison of broad categories.

POPTOP reporter analysis: Synchronized L1s of strains carrying either *POPTOP*, *pop-1(q624)/hT2*, or *POPTOP; rrf-3(pk1426)* were fed on either OP50 or RNAi bacteria for 24 hr at 22°. Early-to-mid L3 animals were scored for mCherry positive cells in the gonad. All images were of equal exposure time (500 msec).

Lineage analysis: Animals were prepared as in Kimble and Hirsh (1979). Briefly, late L2 animals were picked into 2 μl of egg salts on a 5% agar pad. A cover slip with 2 μl OP50 slurry was placed on the slide and was sealed with melted petroleum jelly. Lineage analysis was performed at room temperature (~22°) using a Leica DMZ at ×400 with Nomarski optics. Worms were observed every 20–30 min from L2 molt to mid L3 (~6 hr). The axis of division was assigned with respect to the gonadal proximal/distal axis such that the daughter closer to the linker cell is proximal and the daughter closer to the distal tip cells is distal.

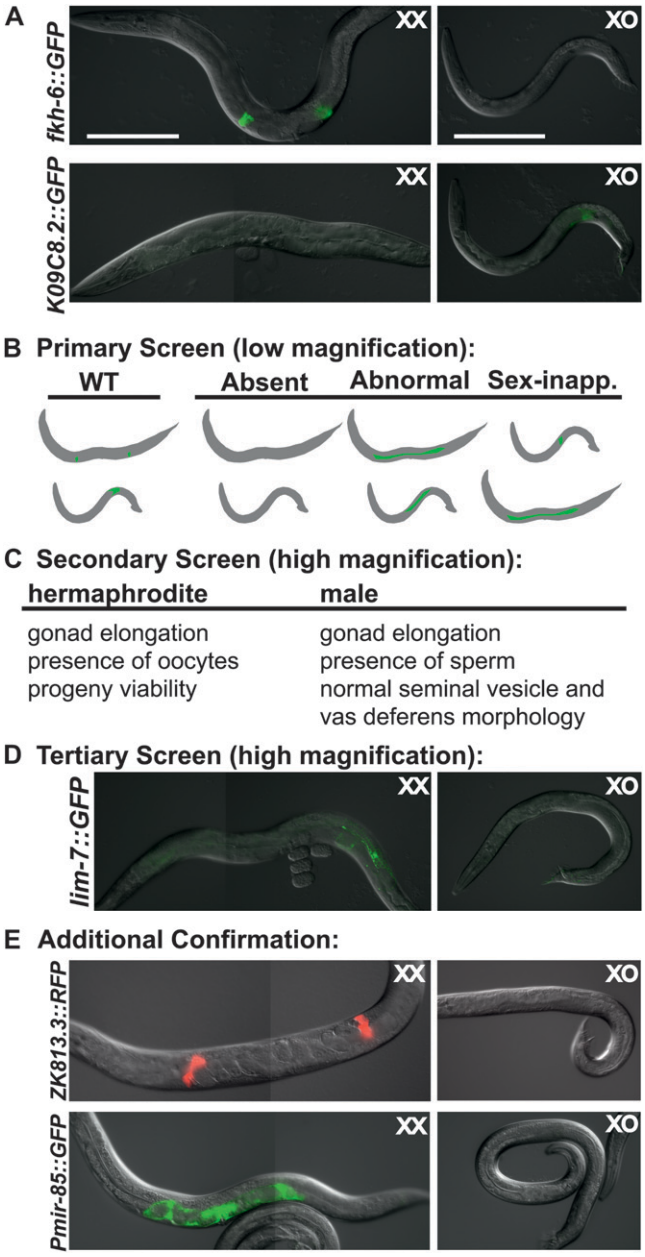

Figure 1.—Genome-wide RNAi screen to identify gonadal defects. (A) Normal expression of GFP reporters used for screen in young adults; strains contained the RNAi hypersensitive mutation *rrf-3(pk1467)* and the high incidence of male mutation *him-8(e1489)*. During L1, *fkh-6::GFP* is expressed in both sexes, but in adults it is expressed only in XX animals. *K09C8.2::GFP* is expressed only in XO animals. Both reporters are expressed only in the somatic gonad. (B) Diagram of reporter gene expression assayed in screen. In the primary screen adults were scored for absent, abnormally patterned, or sex-inappropriate expression of *fkh-6::GFP* and *K09C8.2::GFP* at low magnification. (C) In the secondary screen, animals were scored for gonadal defects by Nomarski optics at high magnification. (D) In the tertiary screen, males were scored for ectopic expression of the sheath marker *lim-7::GFP*, which normally is expressed in the somatic gonad of XX but not XO animals. (E) Additional confirmation of the feminization phenotype employed the hermaphrodite-specific spermatheca marker *ZK813.3::RFP* and the uterine marker *Pmir-85::GFP*. *Pmir-85::GFP* is expressed strongly in uterine cells of XX animals, and expressed very weakly (~100-fold lower) in distal seminal vesicle cells in some males. Only strong expression of *Pmir-85::GFP* (left) was scored as positive. Bars, 200 μm.

RESULTS

A reporter-based RNAi screen for somatic gonad abnormalities in *C. elegans*: To identify genes whose mRNA depletion causes a broad range of gonadal defects in each sex, we performed a multistep RNAi screen, diagrammed in Figure 1. We screened adults from two strains carrying gonad-specific GFP transgenes. The first, *fkh-6::GFP* (Chang *et al.* 2004), is expressed in the gonadal primordium of both sexes during L1, but is hermaphrodite-specific during L4 and adult stages, when it is expressed in spermatheca and sheath cells. The second, *K09C8.2::GFP* (Thoemke *et al.* 2005) is expressed in seminal vesicle and vas deferens cells of the male somatic gonad in late larvae and adults (Figure 1A). Both strains carried the RNAi hypersensitive mutation *rrf-3(pk1426)* (Simmer *et al.* 2002) and the mutation *him-8(e1489)*, which causes a high incidence of males.

The first step was to examine young adult hermaphrodites and males by epifluorescence at low magnification, looking for absent, disorganized, or sex-inappropriate expression of each reporter (Figure 1B). RNAi phenotypes from the primary screen were further characterized by high magnification epifluorescence and DIC microscopy, quantifying marker expression, examining gonadal elongation, tissue organization, presence of oocytes and sperm and, in hermaphrodites, self-fertilization and production of viable offspring (Figure 1C; supporting information, Table S1 and Table S2). RNAi clones causing ectopic expression of *fkh-6::GFP* in adult males were reassayed to confirm feminization of the somatic gonad using the hermaphrodite-specific gonadal sheath cell marker *lim-7::GFP* (Figure 1D; Table S3) and the gene classes chosen for follow-up were further screened for expression of the spermathecal marker *ZK813.3::RFP* and uterine marker *Pmir-85::GFP* (Figure 1E; Table 1).

Classes of gonadal phenotype identified by RNAi: RNAi phenotypes identified in the screen fall into four phenotypic classes, on the basis of visible gonadal morphology and sex-specific reporter expression; examples of each class are shown in Figure 2. The first three classes showed gonadal defects without sex reversal. These are: (1) abnormalities of gonad morphology and GFP expression pattern in both sexes (Figure 2, A and B; 81 genes), (2) hermaphrodites with abnormal pattern of GFP expression and with either normal gonadal morphology (Figure 2, C and D; four genes) or abnormal gonadal morphology (Figure 2, E and F; 27 genes) and with normal male gonads, (3) males with abnormal GFP expression and either normal gonadal morphology (Figure 2, G and H; seven genes) or abnormal gonadal morphology (Figure 2, I and J; 17

TABLE 1

Select genes whose depletion causes male gonadal feminization

Sequence name	Locus	Description	*fkh-6::GFP* sheath/ spermatheca (%)	*n*	*lim-7::GFP* sheath (%)	*n*	*ZK813.3::RFP* spermatheca (%)	*n*	*Pmir-85::GFP* uterine (%)[b]	*n*	Gonadal defects
L4440		Empty vector control	3	187	1	201	0	82	2	163	–
T23D8.9	*sys-1*	Novel β-catenin	70	118	16	152	27	74	72	105	+
W10C8.2	*pop-1*	TCF/LEF transcription factor	73	105	20	117	26	68	28	127	+
W06F12.1	*lit-1*	Serine/threonine kinase	66	116	12	130	19	58	78	112	+
T05G5.3	*cdk-1*	PCTAIRE cyclin-dependent kinase	91	144	14	146	10	83	80	119	+
T06E6.2	*cyb-3*	Cyclin B	26	113	1	136	5	62	62	91	+
C52E4.6	*cyl-1*	Cyclin L	25	118	3	110	0	76	57	152	+
F16B4.8	*cdc-25.2*	M phase inducer phosphatase	53	135	10	144	13	71	86	79	+
M03D4.1	*zen-4*	Kinesin-like protein	32	136	3	104	21	66	48	91	+
B0207.4	*air-2*	Serine/threonine protein kinase	19	134	1	139	3	89	25	107	+
Y39G10AR.13	*icp-1*	Inner centromere protein (INCENP)	9	137	3	147	7	61	23	92	+
C27A2.3	*ify-1*	Predicted securin	21	122	8	92	8	62	27	105	+
K06A5.4	*knl-2*		12	126	1	132	0	69	18	82	+
Y110A7A.1	*hcp-6*	Condensin complex subunit 1	9	138	5	135	3	62	32	92	+
F35B12.5	*sas-5*	Coiled-coil protein	31	159	2	132	9	58	27	122	+
F56A3.4	*spd-2*		18	137	3	145	14	66	25	112	+
C38C10.4[a]	*gpr-2*	G protein regulator/ GoLoco motif	10	144	1	155	4	74	12	114	+
C36E8.5[a]	*tbb-2*	β Tubulin	43	143	2	120	10	60	34	74	+
F58A4.8	*tbg-1*	γ Tubulin	8	181	1	155	3	68	9	133	+
C47B2.3[a]	*tba-2*	α Tubulin	54	150	3	144	13	63	45	112	+

All percentages are the percentage of males that express the hermaphrodite gonad-specific marker indicated.

[a] RNAi clone may target more than one transcript.

[b] Some wild-type *Pmir-85::GFP* males express GFP very weakly in a few distal seminal vesicle cells. All males scored as GFP positive had very bright expression similar to hermaphrodites.

genes) with normal hermaphrodite gonads. The fourth class consisted of feminized males, based on expression of hermaphrodite gonadal markers in males, with or without hermaphrodite gonadal defects (Figure 2, K–M; 67 genes). We found no examples of a fifth anticipated phenotypic class, masculinized hermaphrodites, on the basis of expression of *K09C8.2::GFP*. Further analysis concentrated on the feminized male class, as these genes are particularly likely to help reveal mechanisms of sexual cell fate specification in the somatic gonad.

Genes required for male gonadal cell fates: Among the 67 genes in the feminized male gonad class was, as expected, *fkh-6*, which causes extensive gonadal feminization involving multiple cell types (Chang *et al.* 2004). We also identified the *Abd-B* Hox gene homolog *egl-5*, which has been suggested to be partially feminized on the basis of gonadal morphology (Chisholm 1991). Further analysis of *egl-5* in gonadal development will be presented elsewhere (A. K. Kalis and D. Zarkower, unpublished results). The screen also identified many genes not previously implicated in male/female fate decisions in the gonad, including several components of the gonadal Wnt/β-catenin pathway (Table 1).

To highlight additional pathways and cellular processes required for gonadal development we examined gene ontological (GO) categories of genes identified in the screen. Two categories—cell cycle and cytoskeletal organization—were significantly enriched in the feminized male class relative to the genome as a whole and relative to phenotypic classes in which the male gonad was not feminized (Figure 3). Cell cycle regulators in the feminized male class were *cdk-1*, *cyb-3*, *cyl-1*, and *cdc-25.2*, suggesting a role for cell cycle control in male gonadal differentiation. In the cytoskeletal organization and biogenesis class were a number of genes required for mitotic spindle function and cytokinesis (*e.g.*, *air-2/Aurora B kinase*, *icp-1/INCENP*, *ify-1/SECURIN*, *knl-2*, *hcp-6*, *sas-5*, *spd-2*, *gpr-2*, *zen-4/MKLP1*, and tubulins α, β, and γ), suggesting a critical role for spindle function in male gonadal cell fate specification. The following sections examine the roles of these gene classes in the male somatic gonad.

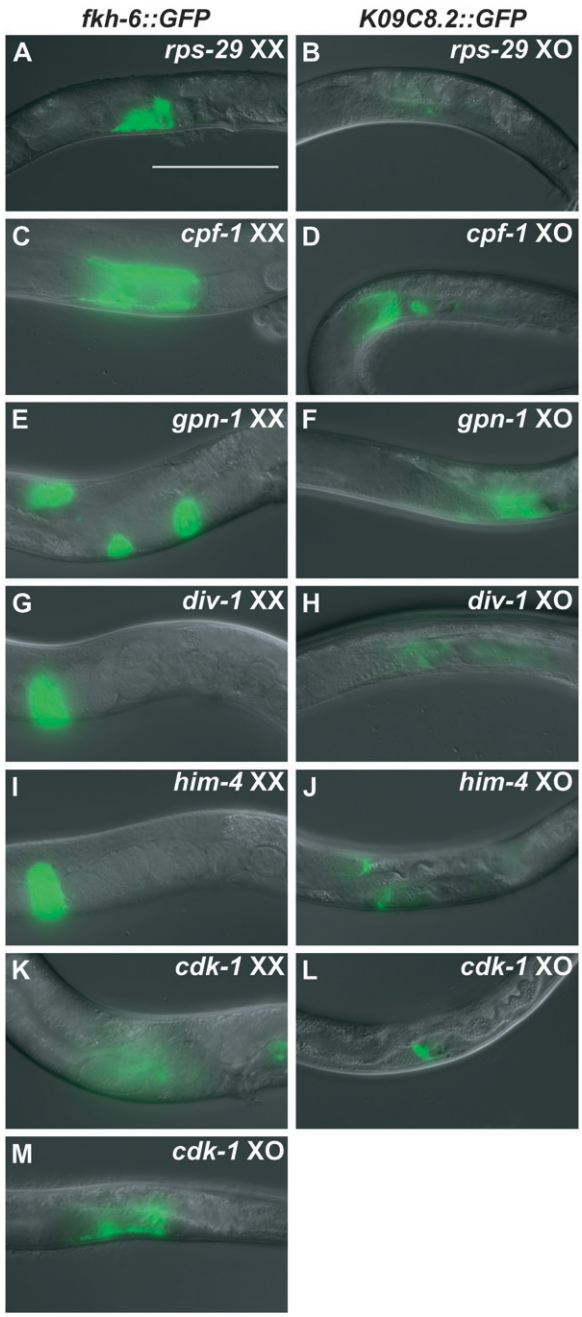

Figure 2.—Classes of gonadal defects identified in RNAi screen. (A and B) *rps-29(RNAi)* exemplifies genes whose depletion causes defects in reporter expression and gonadal morphology in both sexes. (C and D) *cpf-1(RNAi)* causes hermaphrodite-specific abnormalities in reporter expression without apparent defects in gonadal morphology in either sex. (E and F) *gpn-1(RNAi)* causes hermaphrodite-specific defects in reporter expression and gonadal morphology. (G and H) *div-1(RNAi)* causes male-specific abnormalities in reporter expression with apparently normal gonadal morphology in both sexes. (I and J) *him-4(RNAi)* causes male-specific defects in reporter expression and abnormal male gonadal morphology. (K–M) *cdk-1(RNAi)* results in morphological defects in both sexes and sex-inappropriate expression of *fkh-6::GFP* in males. Bar, 100 μm.

A Wnt/β-catenin pathway required for male gonadal cell fates: The feminized male phenotypic class contained the Wnt/β-catenin pathway components *sys-1*, *pop-1*, and *lit-1*, (Table 1), which also are required for asymmetric SGP division in L1 larvae (Siegfried and Kimble 2002; Siegfried *et al.* 2004). *sys-1(q544)* hypomorphic males have normal early gonadal development but highly disorganized adult tissue, suggesting that Wnt/β-catenin pathway activity also functions later in gonadal development (Miskowski *et al.* 2001). Because the role of Wnt/β-catenin signaling after the initial SGP divisions has not been studied and loss of Wnt/β-catenin activity has not been reported to cause gonadal feminization, we first confirmed this feminization in *sys-1* and *pop-1* loss-of-function mutants. Null alleles of both genes are embryonic lethal, necessitating use of hypomorphic mutations (Miskowski *et al.* 2001; Siegfried and Kimble 2002). As expected, *pop-1(q624)* and *sys-1(q544)* males had gonadal defects very similar to those caused by RNAi depletion and expressed multiple hermaphrodite-specific gonadal markers (Figure 4). In addition some mutant males contained gonadal cells with morphology characteristic of hermaphrodite gonadal cell types, particularly sheath cells (Figure 4, D and E) and less frequently uterine cells (Figure 4, J and K). We conclude that loss of *sys-1* and *pop-1* causes extensive gonadal feminization in males.

The Wnt/β-catenin pathway controlling SGP division employs a distinct set of components from those in other tissues (Mizumoto and Sawa 2007). The screen did not identify any components unique to nongonadal Wnt/β-catenin pathways as causing feminization above background, suggesting that the pathway involved in sexual fate specification may be the same one that controls SGP asymmetry. A distinctive feature of the pathway regulating SGP asymmetric division in L1 larvae is the apparent lack of a Wnt ligand (Siegfried *et al.* 2004). To ask whether the pathway controlling later gonadal differentiation requires functional Wnt protein we examined animals mutant for *mig-14/Wntless*, which is required for secretion of Wnt proteins from signaling cells (Banziger *et al.* 2006). We found that *mig-14(ga62)* mutant males have disorganized gonadal morphology but no apparent gonadal feminization (Figure 4C), suggesting that an extracellular Wnt ligand(s) may be involved in gonadal development but is not required for male cell fate determination in the gonad.

Because the Wnt/β-catenin pathway controls asymmetric division of the SGPs, a simple model is that it functions analogously in the male somatic gonad during later differentiation, promoting asymmetric cell divisions that are required for establishment or maintenance of male fates. In this light, it is noteworthy that the male somatic gonad lineage during gonadal elongation and differentiation is composed primarily of asymmetric divisions, whereas most hermaphrodite divisions are symmetrical during this period (Kimble and Hirsh

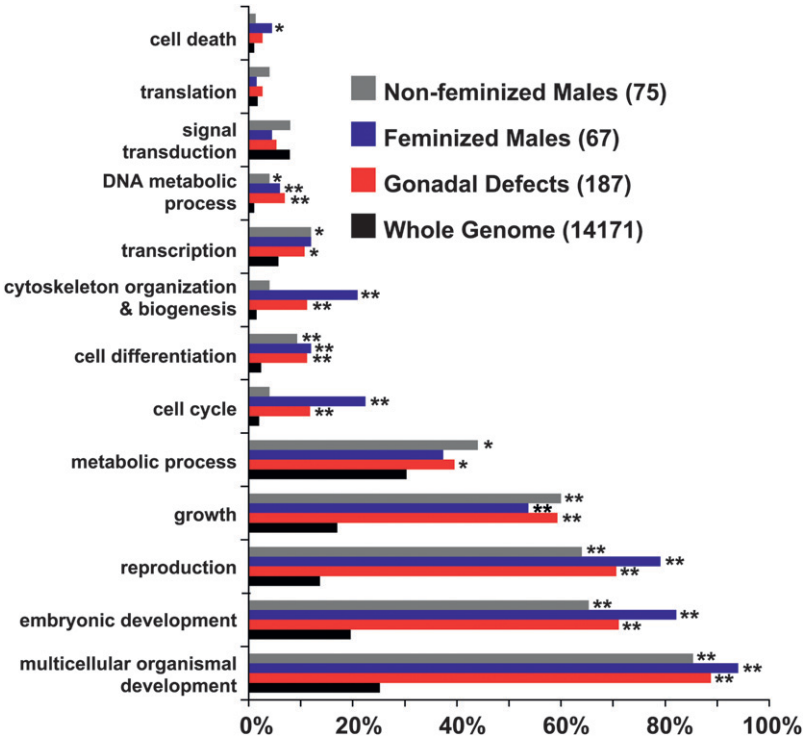

FIGURE 3.—Feminized male phenotypic class is enriched for cytoskeletal and cell cycle genes. Gene ontology (GO) categories were assigned to every gene in each class and "slimmed" to form broad GO categories using GO Term Mapper. Some genes were assigned multiple GO terms. Genes were divided into classes as follows: genes whose depletion caused male gonadal defects without feminization (gray bars), genes whose depletion feminized males (blue bars), all genes detected in the screen (genes whose depletion caused gonadal defects in either sex; red bars), and all genes annotated in RNAi library (black bars). The *X*-axis represents the percentage of genes of each class assigned a particular GO term. χ^2 analyses with Bonferroni corrected *P*-values (*$P < 0.02$ and **$P < 0.003$) were used for statistical comparisons between the whole genome and classes found in the screen.

1979). Feminization of the elongating larval male gonad could result from lack of Wnt/β-catenin pathway activity during this period, but alternatively it could be an indirect consequence of reduced activity earlier in the SGPs. We therefore asked whether the Wnt/β-catenin pathway remains active during gonadal elongation and differentiation and whether elongating male gonads have more cells with Wnt/β-catenin pathway activity than do hermaphrodite gonads at this stage.

To assay Wnt/β-catenin pathway activity we used a transgenic reporter with seven POP-1 binding sites fused to a *pes-10* minimal promoter driving mCherry (POPTOP, **POP**-1 and **T**CF **o**ptimal **p**romoter; GREEN *et al.* 2008). POPTOP expression confirmed that the Wnt/β-catenin pathway remains active after SGP division and males have a higher proportion of gonadal cells with active Wnt/β-catenin signaling than hermaphrodites (Figure 5, A and B). Because the hermaphrodite gonad has about twice as many somatic cells as the male gonad during larval development (42 *vs.* 27 at mid L3), we compared reporter-positive cells per gonadal arm in hermaphrodites to cells per gonad in males. Reporter expression was present in gonadal cells of both sexes during early L3 (Figure 5, C and D) and hermaphrodite gonadal cells consistently had more intense reporter expression than male cells. However, a greater proportion of cells expressed the reporter in males [average of 6.2 in XO ($n = 92$) *vs.* 2.5 in XX ($n = 165$); $P < 0.0001$, paired *t*-test]. The maximum number of mCherry-positive gonadal cells observed correlated closely with the number of asymmetric cell divisions during this stage in each sex: 15 cells in XO (which has 17 asymmetric divisions) *vs.* 5 per gonadal arm in XX (with 6 asymmetric divisions per arm) (Figure 5, A and B). As expected, *pop-1(q624)* and *sys-1(RNAi)* reduced reporter expression in both sexes, confirming the Wnt/β-catenin pathway dependence of the reporter in this tissue. Also, a negative control POPFOP reporter (**POP**-1 **f**ar from **o**ptimal **p**romoter) with mutant POP-1 binding sites (GREEN *et al.* 2008) showed no gonadal expression in either sex ($n = 30$), further confirming the specificity of the reporter expression.

Wnt/β-catenin pathway activity is required for cell division size asymmetry in the elongating male somatic gonad: In the SGPs disruption of the Wnt/β-catenin pathway causes symmetrical divisions, producing daughter cells of approximately equal size. We asked whether this also is the case in the elongating male somatic gonad, using the viable *sys-1* loss-of-function allele *sys-1(q544)*. We focused on division of the three vas deferens precursor cells, which normally undergo a series of asymmetric divisions starting at the L2 molt in which the size of the resulting daughter cells is radically different. In *sys-1(q544)* mutants, these divisions often produced daughter cells with little or no size asymmetry and had a lengthened cell cycle (Figure 6, A–C). We conclude that the Wnt/β-catenin pathway controls cell division size asymmetry and the rate of mitosis in the elongating male somatic gonad.

Cell cycle regulators *cdk-1* and *cyb-3* activate Wnt/β-catenin signaling to promote male gonadal cell fates: Among cell cycle regulators required for male gonadal

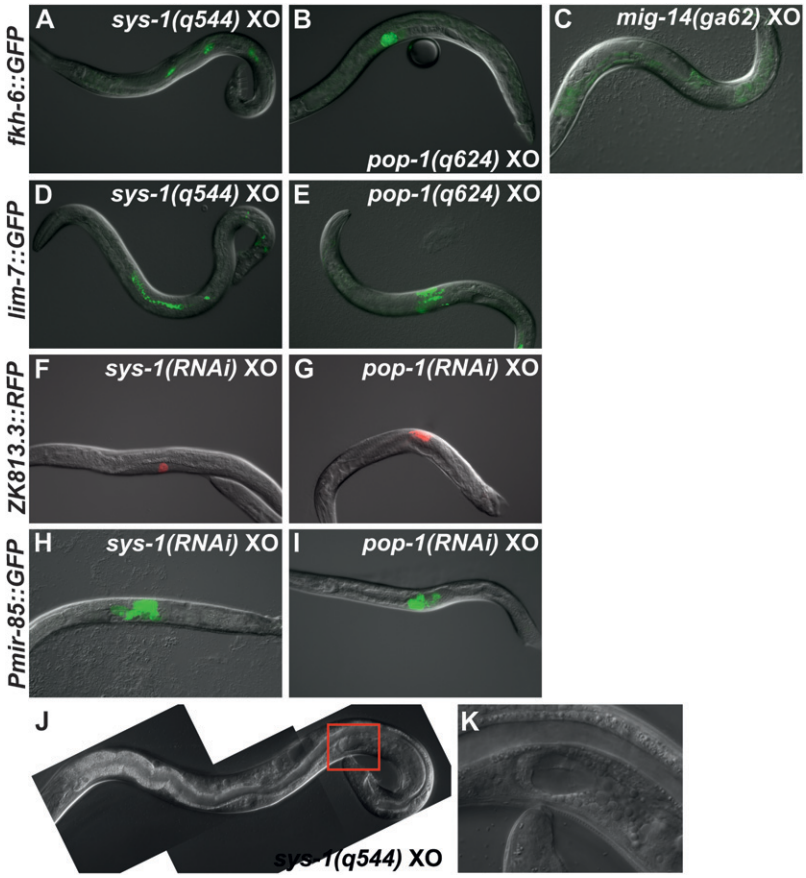

FIGURE 4.—Loss-of-function mutations and RNAi depletion of Wnt/β-catenin pathway genes feminize the male somatic gonad. (A) *sys-1(q544)* males express the hermaphrodite spermatheca and sheath marker *fkh-6::GFP* (87%, $n = 54$). (B) *pop-1(q624)* hypomorphic mutants express *fkh-6::GFP* (15%, $n = 78$). (C) *mig-14(ga62)* young adult mutant males, which are defective in Wnt ligand secretion, do not express *fkh-6::GFP* (3%, $n = 87$) in the somatic gonad (green background is intestinal autofluorescence). (D) *sys-1(q544)* males express the sheath marker *lim-7::GFP* (65%, $n = 103$). (E) *pop-1(q624)* males express *lim-7::GFP* (17%, $n = 36$). (F) *sys-1(RNAi)* males express the spermatheca marker *ZK813.3::RFP* (27%, $n = 74$; also shown in Table 1). (G) *pop-1(RNAi)* males express *ZK813.3::RFP* (26%, $n = 68$). (H) *sys-1(RNAi)* males express the uterine marker *Pmir-85::GFP* (72%, $n = 105$). (I) *pop-1(RNAi)* males express *Pmir-85::GFP* (28%, $n = 127$). (J and K) Some *sys-1(q544)* males (<5%) have uterine tissue identifiable by morphology alone. (Red square in J indicates region magnified in K.)

fates were the cyclin-dependent kinase *cdk-1* and its cognate cyclin *cyb-3* (Figure 2, K–M; Table 1). Previous work showed that the G1/S cell cycle regulator *cyd-1* activates expression of FKH-6, coupling early male gonadal differentiation to the mitotic cell cycle (TILMANN and KIMBLE 2005). The requirement for *cdk-1* and *cyb-3* suggests another cell cycle link to male gonadal differentiation. CDK-1 is a CDC2 homolog that regulates the prophase/metaphase transition and functions in meiotic maturation (SHIRAYAMA *et al.* 2006). We confirmed the feminization phenotype of *cdk-1* using the temperature-sensitive allele *cdk-1(ne2257)*, finding that *ne2257*

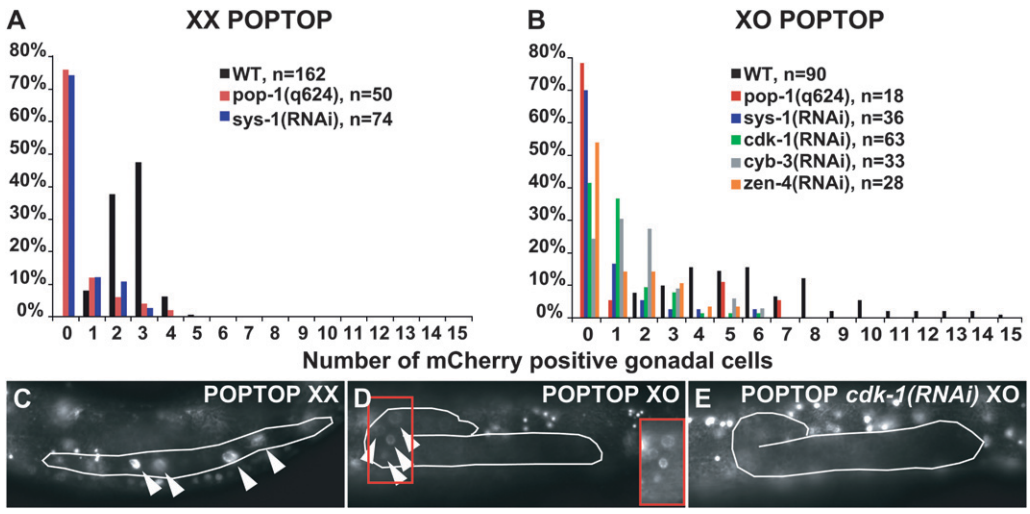

FIGURE 5.—Gonadal Wnt/β-catenin pathway activity differs between sexes and requires cell cycle and mitotic spindle regulators. (A and B) Histograms of number of gonadal cells with *POPTOP* Wnt/β-catenin reporter activity from early through mid L3. (A) Number of reporter-expressing cells per gonadal arm in hermaphrodites. (B) Number of reporter-expressing cells per male gonad. (C) *POPTOP* expression in wild-type hermaphrodite L3 gonad (outlined). (D) *POPTOP* expression in wild-type male L3 gonad. Inset image, indicated by red rectangle, shows reporter positive cells at greater brightness. (E) *POPTOP* expression in *cdk-1(RNAi)* L3 male gonad is greatly reduced, with no positive gonadal cells visible in this animal (background is from expression in neighboring tissues).

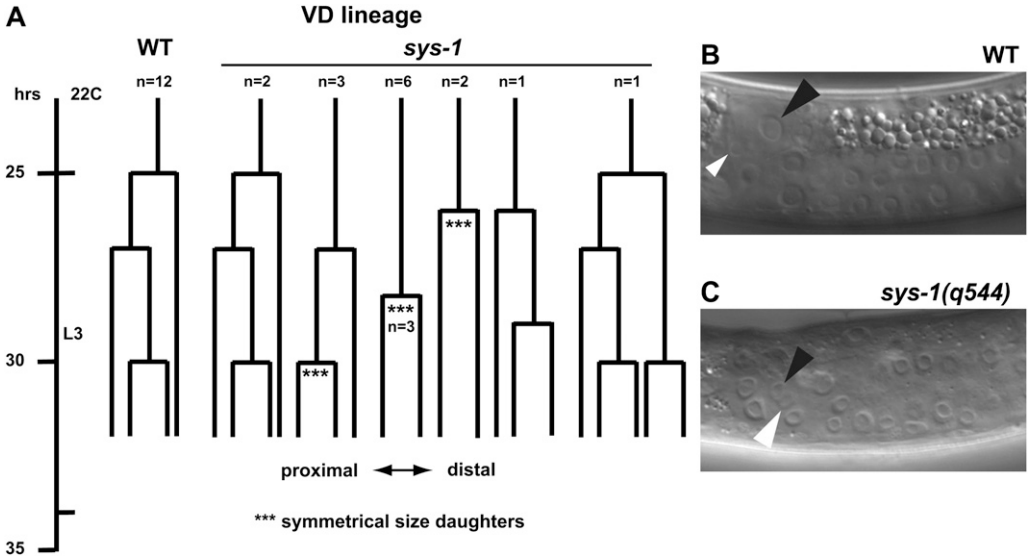

FIGURE 6.—Symmetric and delayed divisions of vas deferens (VD) precursor cells in *sys-1* mutant males. (A) Lineage of VD precursor cells during the L3 somatic gonadal proliferative stage. Lineages were followed from the L2 molt until just after mid L3 when cell divisions in this lineage become difficult to discern. In *sys-1(q544)* mutants VD divisions were usually delayed and were symmetrical with respect to daughter cell size where indicated (***). (B and C) Examples of VD precursor cell division. Black arrowhead indicates VD.p and white arrowhead indicates VD.d. (Plane of division is relative to the gonadal axis rather than body axis). (B) In wild type the first division of the VD precursor cell results in a much larger VD.p daughter and a much smaller VD.d daughter. (C) *sys-1* mutant male in which the VD precursor has just completed division, forming VD.p and VD.d daughters of equal size.

males at restrictive temperature exhibit gonadal feminization similar to that caused by *cdk-1* RNAi (data not shown).

We next asked whether the feminization of *cdk-1*(RNAi) males is due to a requirement in gonadal cell fate determination at the SGP stage or reflects a later function. On the basis of expression of *lag-2::GFP* and *ceh-22::GFP* and examination of cell morphology, L2 *cdk-1(RNAi)* males had normal numbers of linker cells and distal tip cells, indicating that the early male gonadal lineages were largely unaffected (Figure S1). This suggests that *cdk-1* is required after SGP formation and division to establish or maintain male gonadal cell fates.

In the first zygotic cell cycle CDK-1 acts with other kinases to control the oocyte-to-embryo transition by destroying the zinc finger protein OMA-1. This allows activation of asymmetrically distributed cell fate determinants partitioned during the first mitotic division, thereby coupling mitosis to cell fate determination (SHIRAYAMA *et al.* 2006). We asked whether *cdk-1* couples the cell cycle to male gonadal differentiation by a similar mechanism. To test whether the kinases that act with CDK-1 in the first zygotic cell cycle also are required for male gonadal cell fate determination, we depleted GSK-3, KIN-19, and MBK-2. In each case, RNAi of embryos gave sterile adults, confirming the effectiveness of the depletion, but we observed no feminization of the male gonad (data not shown).

Since CDK-1 controls the first zygotic cell cycle via destruction of OMA-1, we considered the possibility that CDK-1 might act via OMA-1 destruction in the male gonad, albeit independently of *gsk-3*, *kin-19*, and *mbk-2*. We used RNAi to deplete *cdk-1* together with *oma-1* and its paralog *oma-2*, asking whether, as in embryos, their co-depletion can suppress loss of *cdk-1*. RNAi of *oma-1/2* alone caused the expected block in meiotic maturation in XX animals, but male somatic gonad feminization in animals depleted for *cdk-1* together with *oma-1/2* was not reduced relative to *cdk-1* RNAi alone (Figure S2, A–C). The *oma-1* gain-of-function allele *zu405* blocks the oocyte-to-embryo transition similarly to *cdk-1* loss of function (SHIRAYAMA *et al.* 2006). We examined adult male gonads in *zu405* mutants, but observed no defects in male gonadal morphology or ectopic expression of *fkh-6::GFP* (Figure S2 D). From these results we conclude that *cdk-1* function in the male somatic gonad does not involve OMA-1 destruction.

In the zygote, CDK-1-mediated destruction of OMA-1 indirectly activates Wnt signaling (SHIRAYAMA *et al.* 2006). Although our data indicated that the gonadal function of *cdk-1* is mechanistically distinct from its early zygotic function, the *cdk-1(RNAi)* male gonadal phenotype closely resembles that of Wnt/β-catenin pathway mutants. We therefore considered the possibility that *cdk-1* regulates the Wnt/β-catenin pathway during male gonadal differentiation independently of *oma-1*. Indeed, *cdk-1(RNAi)* males and hermaphrodites had almost no POPTOP activity in the larval somatic gonad (Figure 5, B and E; data not shown). Depletion of *cyb-3* also caused reduced POPTOP activity (Figure 5B), suggesting that CDK-1 regulation of Wnt/β-catenin signaling may be cyclin dependent. We conclude that *cdk-1* activates Wnt/β-catenin signaling in the somatic gonad, but by a mechanism distinct from that used in the early zygote.

The mitotic spindle regulator *zen-4* is required for Wnt/β-catenin pathway activity in the somatic gonad: A third group of genes identified in the feminized male category encodes a variety of proteins required for

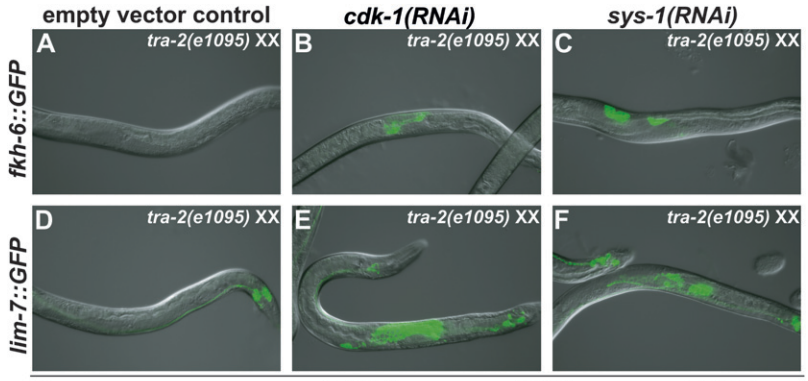

G

	control RNAi		sys-1 RNAi		cdk-1 RNAi	
	% GFP+ male gonads	n	% GFP+ male gonads	n	% GFP+ male gonads	n
him-8; fkh-6::GFP	0	115	22	112	54	109
tra-2(ar221ts); fkh-6::GFP	5	152	60	85	50	101
tra-2(e1095); fkh-6::GFP	3	96	57	96	83	109
tra-1(e1099); fkh-6::GFP	25	168	46	142	43	81
him-8; lim-7::GFP	1	129	12	132	1	120
tra-2(ar221ts); lim-7::GFP	9	283	66	103	32	79
tra-2(e1095); lim-7::GFP	1	88	27	62	27	77
tra-1(e1099); lim-7::GFP	15	108	38	101	7	175

FIGURE 7.—Male gonadal feminization does not require the global sex determination pathway. Expression of *fkh-6::GFP* spermatheca marker (A–C) and *lim-7::GFP* sheath marker (D–F) in *tra-2(e1095)* XX pseudomales. (A–C) *tra-2(e1095)* mutants hatched onto control RNAi seldom expressed *fkh-6::GFP*, but when hatched onto *cdk-1* or *sys-1* RNAi they frequently expressed *fkh-6::GFP* (quantitated in G). (D–F) *tra-2(e1095)* XX pseudomales on control RNAi seldom expressed *lim-7::GFP*, but when raised on *cdk-1* or *sys-1* RNAi they frequently expressed *lim-7::GFP*. [*lim-7::GFP* expression visible in control RNAi (D) is in the tail and other nongonadal tissues.] (G) Feminization due to *sys-1* or *cdk-1* RNAi also was not blocked by *tra-2(ar221ts)* at the restrictive temperature or by *tra-1(e1099)*.

normal formation and regulation of the mitotic spindle (Table 1). Because the RNAi phenotype of these genes resembled that caused by depletion of Wnt/β-catenin pathway components, we asked whether they might be required for the activity of the Wnt/β-catenin pathway in the somatic gonad. We focused on the kinesin-related protein ZEN-4, a component of the centrospindlin complex that constructs the mitotic spindle midzone and is required for microtubule bundling and completion of cytokinesis (MISHIMA *et al.* 2002). ZEN-4 is phosphorylated by the AIR-2/Aurora B kinase, and this phosphorylation is required for efficient completion of cytokinesis (GUSE *et al.* 2005). *zen-4* RNAi caused reduced POPTOP expression in gonads of both sexes during L3 (Figure 5B), indicating that the requirement for *zen-4* in male gonadal fate specification results at least in part from a requirement in Wnt/β-catenin signaling. It is likely, on the basis of the similarity in gonadal phenotypes and their known interactions, that other regulators of the mitotic spindle identified in the screen also are required for Wnt/β-catenin activity.

Sex reversal of male gonadal cells in larvae does not require the global sex determination pathway: Temperature shift experiments using conditional alleles of the global sex determining genes *tra-2* and *fem-1* have shown that the global sex determination pathway is necessary prior to hatching for proper gonadal sex determination and is no longer required after division of the SGPs (KLASS *et al.* 1976; NELSON *et al.* 1978). It therefore is likely that the feminization caused by larval depletion of Wnt/β-catenin pathway components and *cdk-1* results from defects independent of the global pathway. However a plausible alternative is that reduced Wnt/β-catenin signaling in males inappropriately activates the global pathway. To help distinguish between these possibilities, we asked whether the feminizing genes *tra-1* and *tra-2* are required for male gonadal feminization caused by depletion of *sys-1* and *cdk-1*. During normal hermaphrodite development, *tra-1* and *tra-2* are required for feminization of all tissues including the somatic gonad and at restrictive temperature *tra-2(ar221ts)* XX animals develop as almost fully masculinized pseudomales (HODGKIN 2002). TRA-1 also is required for male gonadal development, and *tra-1(null)* XX animals develop as pseudomales with variably abnormal gonads (HODGKIN 1987). We treated wild-type, *tra-1(e1099)*, *tra-2(e1095)*, and *tra-2(ar221ts)* XX animals with *sys-1* or *cdk-1* RNAi. Null mutations in *tra-1* or *tra-2* did not eliminate feminization due to *sys-1* or *cdk-1* RNAi, indicating that both genes are dispensable. *tra-1(e1099)* pseudomales also had elevated expression of both reporters in the absence of RNAi, suggesting that loss of *tra-1* incompletely masculinizes the somatic gonad (Figure 7). We conclude from these results that feminization due to loss of Wnt/β-catenin signaling occurs independently of *tra-1* and *tra-2* and likely also the rest of the global sex determination pathway.

DISCUSSION

We have performed a reporter-based genome-wide RNAi screen to find genes required for normal gonadal development in each sex. The screen involved several steps of analysis using highly specific GFP reporter

genes and identified >200 genes necessary for normal expression of the gonadal reporters, normal gonadal morphology, or both. Most of these genes are required in both sexes, but the screen identified about 30 genes whose depletion affected only the hermaphrodite gonad and a similar number whose depletion affected only males. The screen identified almost 70 genes whose depletion feminized the male gonad but, as discussed below, none that caused gonadal masculinization in hermaphrodites. To learn more about mechanisms of male gonadal fate specification we focused on genes in the feminized male category involved in Wnt/β-catenin signaling, cell cycle control, and mitotic spindle function.

Genome-wide RNAi to identify gonadal regulators: The screen relied on RNAi depletion posthatching, which has both advantages and disadvantages. The primary advantage of this strategy is its ability to identify many genes that are essential for embryonic viability and thus difficult or impossible to identify using maternal RNAi depletion or forward genetics. Also, using GFP reporters allowed the identification of many genes whose depletion did not cause obvious morphological defects but severely affected expression of cell fate markers. The genes identified should comprise a large subset of those required for gonadal development in either sex. Nevertheless, there are important caveats. First, many genes doubtless were not detected, because the RNAi library does not target all genes and because some genes are not susceptible to feeding RNAi. As examples, we did not detect all members of some known protein complexes such as SWI-SNF. Second, RNAi depletion is often incomplete; although this allows identification of genes required for embryonic viability (*e.g.*, *sys-1*, *pop-1*, *etc.*), it also means that many phenotypes we found are likely to be hypomorphic. Third, because the gonadal primordium forms prior to hatching, a specific class of genes likely to be underrepresented in the screen are those required very early in gonadogenesis. We did identify genes involved in early SGP development (*e.g.*, *fkh-6*), but missed others (*e.g.*, *hnd-1*, *ehn-3*, and *tra-1*), either because they were not represented in the library or are required too early to be effectively targeted by our strategy. Despite these caveats, this screen complements prior genetic screens and greatly extends the repertoire of known gonadal regulators.

Male *vs.* female gonadal differentiation: The screen identified many genes whose depletion caused male-to-female gonadal cell fate transformations. The conclusion that these gonads were feminized was based on the ectopic expression of up to four hermaphrodite-specific reporters (Table 1), typical sheath cell morphology for cells expressing *lim-7::gfp* and presence of uterine-appearing tissue (Figure 4). This reversal of sexual fate strongly implies that male gonadal differentiation requires active suppression of a regulatory program promoting hermaphrodite fates. Analysis of *tra-1* and *tra-2* mutants suggested that this program does not involve the global sex determination pathway, consistent with previous work showing that the global pathway is required in the gonad only earlier in development (Klass *et al.* 1976; Nelson *et al.* 1978). The screen also identified many genes whose depletion caused male gonadal defects but not feminization, which suggests that female fates are not triggered simply by abnormalities in male gonadal development; instead, male gonadal cells apparently require a specific regulatory program to override hermaphrodite development.

Our results also suggest that sexual fates remain plastic in the male gonad during larval development. Recent work in the mouse found that adult ovarian cells can transdifferentiate into testicular cells when the sexual regulator *Foxl2* is conditionally deleted (Uhlenhaut *et al.* 2009), and thus plasticity of sexual fate after primary sex determination appears to be a feature of both vertebrate and invertebrate gonadal cells.

Some genes in the feminized male category (RNA polII, snRNP-associated proteins) are general regulators of gene expression that seem unlikely candidates to control sexual fate specification. We speculate that their partial RNAi depletion indirectly affects other genes with more specific roles in this process and sensitivity to altered expression levels.

Most of the genes in the feminized male category also were required for normal gonadal development in hermaphrodites. A simple interpretation is that these genes are components of a common developmental program shared by both sexes but modified in males to function sex specifically, much as proposed previously on the basis of cell lineage analysis (Kimble and Hirsh 1979). How is this shared gonadal program modified to promote male cell fates? The best characterized gonadal masculizing gene is *fkh-6*, but it is expressed in males only during L1 and does not cause full sex reversal (Chang *et al.* 2004) and hence other masculinizing genes must be involved. The RNAi screen did find other genes with male-specific gonadal phenotypes. These are candidates to impose sex specificity on the common gonadal program and indeed one of them, *egl-5*, is required for sex-specific POP-1 activity (A. K. Kalis and D. Zarkower, unpublished results).

The screen did not detect genes whose depletion caused female-to-male transformations in XX animals. Likewise, forward genetic screens have identified genes causing feminization of the male gonad, but not the reverse (excepting global sex determination genes such as *tra-1* and *tra-2*) (Chang *et al.* 2004, 2005; Tilmann and Kimble 2005). This difference suggests one of two possibilities. First, disrupting sexual differentiation may cause male but not hermaphrodite gonadal cells to adopt fates appropriate to the other sex. Alternatively, our screen might have been unable to detect masculinization of the XX gonad. The reporters used in this screen can readily detect XX gonadal masculinization caused by ectopic EGL-5 expression (A. K. Kalis and D.

Zarkower, unpublished results), favoring the view that disruption of gonadal differentiation has different consequences in the two sexes. However, we cannot exclude the possibility that disrupting female gonadal differentiation can result in male fates but this screen missed the relevant genes due to incompleteness of the RNAi library, genetic redundancy, maternal effects, or other factors.

Wnt/β-catenin signaling and sexual fate: Previous work showed that a Wnt/β-catenin pathway is required in the SGPs of both sexes for asymmetric cell fate specification (Siegfried and Kimble 2002). Here we show that Wnt/β-catenin signaling also is required in both sexes after the first SGP division and is necessary for the specification and/or maintenance of male gonadal cell fates. Wnt/β-catenin signaling is required for many aspects of development in *C. elegans*, including differentiation of sexually dimorphic cell lineages in the male tail and hermaphrodite vulva (Sternberg 2005; Wu and Herman 2006, 2007; Yu *et al.* 2009). In contrast to its roles in these other tissues, loss of Wnt/β-catenin signaling in the male gonad not only compromises sexual differentiation but also causes the adoption of cell fates appropriate to the opposite sex.

Wnt/β-catenin signaling also is critical for specifying sexual identity in gonadal cells of arthropods and vertebrates (Kim and Capel 2006; Defalco *et al.* 2008), and in principle this might represent an ancient and conserved role in gonadal sex determination. Confounding this view are major differences in how Wnt/β-catenin signaling is deployed in the species that have been examined. For example, in Drosophila male-specific gonadal pigment cells are derived from extragonadal tissues and are induced by Wnt2 produced by the gonad (Defalco *et al.* 2008), whereas in mice *Wnt4* is required for gonadal sex determination only in females (Kim and Capel 2006). Unlike in flies and mice, *C. elegans* gonadal Wnt/β-catenin pathway activity is required in both sexes within the somatic gonad primordium and does not appear to involve a Wnt ligand. On the basis of these differences it seems likelier that Wnt/β-catenin signaling has been independently recruited to help specify gonadal cell fates in these three phyla.

Cell cycle regulators and control of gonadal Wnt/β-catenin signaling: Canonical Wnt pathways can be controlled by the availability of Wnt ligand, but the gonadal Wnt/β-catenin pathway appears not to require such a ligand, or at least its secretion. How then is Wnt/β-catenin signaling regulated in the developing somatic gonad? Part of the answer is the G2/M regulators *cdk-1* and *cyb-3*, which we found are required for Wnt/β-catenin activity. The G1/S regulator *cyd-1/cyclin D* acts analogously in the SGPs to control asymmetric cell division, *fkh-6* expression, and Wnt/β-catenin function, and has been proposed to link these processes to mitotic progression (Tilmann and Kimble 2005). The G1/S regulators *cye-1/cyclin E* and *cdk-2* also play an important role in the early SGP lineage: their asymmetrical expression, regulated by the Wnt/MAPK pathway, is required to distinguish fates of the DTCs from those of their sister cells (Fujita *et al.* 2007). Our results indicate that *cdk-1* helps connect asymmetric cell division, Wnt/β-catenin activity, and cell fate determination. This may help link these processes to the gonadal cell cycle or, alternatively, *cdk-1* may act independently from its cell cycle function. There are precedents for both modes of regulation: in the Drosophila nervous system, Cdk1 contributes to asymmetric division of sensory organ precursors via a role in cell cycle control (Fichelson and Gho 2004), but in neuroblasts Cdk1 controls spindle positioning and asymmetric cell division separately from its role in cell cycle progression (Tio *et al.* 2001). In the nematode gonad defects in the Wnt/β-catenin pathway apparently compromise cell cycle progression, as we found that *sys-1* mutant cells have greatly delayed mitotic divisions. It is unclear whether this represents a direct effect on cell cycle control or an indirect effect, for example via a mitotic spindle checkpoint. Either way, it is clear that Wnt/β-catenin activity is coupled to cell cycle progression in the somatic gonad.

In *C. elegans*, *cdk-1* promotes Wnt/β-catenin activity in the first zygotic cell cycle via a mechanism involving the *gsk-3*, *mbk-2*, and *kin-19* kinases and requiring OMA-1 degradation (Shirayama *et al.* 2006). We find that these kinases and OMA-1 are not involved in gonadal regulation of Wnt/β-catenin signaling by *cdk-1*. Thus CDK-1 activates Wnt/β-catenin signaling in the somatic gonad, but via a different regulatory network from that employed in the zygote. To further define the role of *cdk-1* in male gonadal fate determination it will be important to identify the targets of CDK-1 phosphorylation in the somatic gonad and to look for additional shared components between the zygotic and gonadal Wnt/β-catenin stimulating mechanisms.

The mitotic apparatus and gonadal sex determination: Why does depletion of spindle/cytokenesis regulators cause gonadal feminization? We found that POPTOP reporter activity is severely reduced by *zen-4* RNAi, suggesting that proper spindle function is necessary for Wnt/β-catenin activity. ZEN-4 is an AIR-2/Aurora B kinase target that is a component of the spindle midbody and is required for efficient cytokinesis (Severson *et al.* 2000). ZEN-4 also plays an apparently distinct role in cell polarity in postmitotic cells of the pharynx (Portereiko *et al.* 2004). The requirement for ZEN-4 could stem from either of these functions. It appears more likely, however, that ZEN-4 functions in male cell fate determination via its mitotic spindle function, because depletion of *air-2* and a number of other spindle regulators caused similar feminization of the male somatic gonad.

Several of the spindle regulators identified in the RNAi screen have been shown to be required for spindle

asymmetry and asymmetric cell division, and even nonspecific spindle disruption can cause delayed spindle displacement or symmetrical division (Tsou *et al.* 2003; Labbe *et al.* 2004; Gonczy 2008; McCarthy Campbell *et al.* 2009). It therefore seems likely that the feminization caused by depletion of spindle regulators stems from a defect in cell division asymmetry, similar to that observed in Wnt/β-catenin pathway mutants. We were unable to confirm this by direct observation of spindle asymmetry during larval development, due to rapid division and small size of the somatic gonad cells. Nevertheless, one can envision at least two potential roles for spindle asymmetry in male fate determination, which are not mutually exclusive. First, failure or delay of spindle asymmetry may prevent necessary asymmetric distribution of male fate determinants in daughter cells. Second, defects in asymmetric spindle establishment may lead to symmetrical distribution of one or more normally asymmetric Wnt/β-catenin pathway components, preventing the functional interaction of the Wnt/β-catenin pathway with male fate determinants.

Our data indicate essential roles for the cell cycle, the mitotic spindle, and a gonadal Wnt/β-catenin pathway in male fate determination. It will be important in the future to dissect the relationships between these processes. It also will be important to identify the male determinants that impart sex specificity on the common gonadal program and to further elucidate the molecular interactions between the large and diverse groups of gonadal regulators identified in the screen.

The authors thank Judith Kimble and David Greenstein for helpful discussions and for sharing strains and reagents. We also thank Jennifer Ross Wolff and members of the Zarkower lab for discussions and critical reading of the manuscript and Matthew Berkseth for technical assistance. Many strains used in this work were provided by the Caenorhabditis Genetics Center, which is funded by the National Institutes of Health (NIH) National Center for Research Resourses (NCRR). This work was supported by NIH grants GM53099 (to D.Z.) and T32HD007480 (to A.K.K.).

LITERATURE CITED

Banziger, C., D. Soldini, C. Schutt, P. Zipperlen, G. Hausmann *et al.*, 2006 Wntless, a conserved membrane protein dedicated to the secretion of Wnt proteins from signaling cells. Cell **125:** 509–522.

Chang, W., C. Tilmann, K. Thoemke, F. H. Markussen, L. D. Mathies *et al.*, 2004 A forkhead protein controls sexual identity of the C. elegans male somatic gonad. Development **131:** 1425–1436.

Chang, W., C. E. Lloyd and D. Zarkower, 2005 DSH-2 regulates asymmetric cell division in the early C. elegans somatic gonad. Mech. Dev. **122:** 781–789.

Chisholm, A., 1991 Control of cell fate in the tail region of C. elegans by the gene egl-5. Development **111:** 921–932.

DeFalco, T., N. Camara, S. Le Bras and M. Van Doren, 2008 Nonautonomous sex determination controls sexually dimorphic development of the Drosophila gonad. Dev. Cell **14:** 275–286.

Fichelson, P., and M. Gho, 2004 Mother-daughter precursor cell fate transformation after Cdc2 down-regulation in the Drosophila bristle lineage. Dev. Biol. **276:** 367–377.

Fujita, M., H. Takeshita and H. Sawa, 2007 Cyclin E and CDK2 repress the terminal differentiation of quiescent cells after asymmetric division in C. elegans. PLoS One **2:** e407.

Gonczy, P., 2008 Mechanisms of asymmetric cell division: flies and worms pave the way. Nat. Rev. Mol. Cell. Biol. **9:** 355–366.

Green, J. L., T. Inoue and P. W. Sternberg, 2008 Opposing Wnt pathways orient cell polarity during organogenesis. Cell **134:** 646–656.

Guse, A., M. Mishima and M. Glotzer, 2005 Phosphorylation of ZEN-4/MKLP1 by aurora B regulates completion of cytokinesis. Curr. Biol. **15:** 778–786.

Harris, M. A., J. Clark, A. Ireland, J. Lomax, M. Ashburner *et al.*, 2004 The Gene Ontology (GO) database and informatics resource. Nucleic Acids Res. **32:** D258–D261.

Hirsh, D., D. Oppenheim and M. Klass, 1976 Development of the reproductive system of Caenorhabditis elegans. Dev. Biol. **49:** 200–219.

Hodgkin, J., 1987 A genetic analysis of the sex-determining gene, tra-1, in the nematode Caenorhabditis elegans. Genes Dev. **1:** 731–745.

Hodgkin, J., 2002 Exploring the envelope. Systematic alteration in the sex-determination system of the nematode caenorhabditis elegans. Genetics **162:** 767–780.

Hubbard, E. J., and D. Greenstein, 2000 The Caenorhabditis elegans gonad: a test tube for cell and developmental biology. Dev. Dyn. **218:** 2–22.

Kamath, R. S., and J. Ahringer, 2003 Genome-wide RNAi screening in Caenorhabditis elegans. Methods **30:** 313–321.

Kim, Y., and B. Capel, 2006 Balancing the bipotential gonad between alternative organ fates: a new perspective on an old problem. Dev. Dyn. **235:** 2292–2300.

Kimble, J., and D. Hirsh, 1979 The postembryonic cell lineages of the hermaphrodite and male gonads in Caenorhabditis elegans. Dev. Biol. **70:** 396–417.

Klass, M., N. Wolf and D. Hirsh, 1976 Development of the male reproductive system and sexual transformation in the nematode Caenorhabditis elegans. Dev. Biol. **52:** 1–18.

Labbe, J. C., E. K. McCarthy and B. Goldstein, 2004 The forces that position a mitotic spindle asymmetrically are tethered until after the time of spindle assembly. J. Cell Biol. **167:** 245–256.

McCarthy Campbell, E. K., A. D. Werts and B. Goldstein, 2009 A cell cycle timer for asymmetric spindle positioning. PLoS Biol. **7:** e1000088.

Mishima, M., S. Kaitna and M. Glotzer, 2002 Central spindle assembly and cytokinesis require a kinesin-like protein/RhoGAP complex with microtubule bundling activity. Dev. Cell **2:** 41–54.

Miskowski, J., Y. Li and J. Kimble, 2001 The sys-1 gene and sexual dimorphism during gonadogenesis in Caenorhabditis elegans. Dev. Biol. **230:** 61–73.

Mizumoto, K., and H. Sawa, 2007 Cortical beta-catenin and APC regulate asymmetric nuclear beta-catenin localization during asymmetric cell division in C. elegans. Dev. Cell **12:** 287–299.

Nelson, G. A., K. K. Lew and S. Ward, 1978 Intersex, a temperature-sensitive mutant of the nematode Caenorhabditis elegans. Dev. Biol. **66:** 386–409.

Phillips, B. T., and J. Kimble, 2009 A new look at TCF and beta-catenin through the lens of a divergent C. elegans Wnt pathway. Dev. Cell **17:** 27–34.

Portereiko, M. F., J. Saam and S. E. Mango, 2004 ZEN-4/MKLP1 is required to polarize the foregut epithelium. Curr. Biol. **14:** 932–941.

Severson, A. F., D. R. Hamill, J. C. Carter, J. Schumacher and B. Bowerman, 2000 The aurora-related kinase AIR-2 recruits ZEN-4/CeMKLP1 to the mitotic spindle at metaphase and is required for cytokinesis. Curr. Biol. **10:** 1162–1171.

Shirayama, M., M. C. Soto, T. Ishidate, S. Kim, K. Nakamura *et al.*, 2006 The conserved kinases CDK-1, GSK-3, KIN-19, and MBK-2 promote OMA-1 destruction to regulate the oocyte-to-embryo transition in C. elegans. Curr. Biol. **16:** 47–55.

Siegfried, K. R., and J. Kimble, 2002 POP-1 controls axis formation during early gonadogenesis in C. elegans. Development **129:** 443–453.

Siegfried, K. R., A. R. Kidd, III, M. A. Chesney and J. Kimble, 2004 The sys-1 and sys-3 genes cooperate with Wnt signaling to establish the proximal-distal axis of the Caenorhabditis elegans gonad. Genetics **166:** 171–186.

Simmer, F., M. Tijsterman, S. Parrish, S. P. Koushika, M. L. Nonet *et al.*, 2002 Loss of the putative RNA-directed RNA polymerase

RRF-3 makes C. elegans hypersensitive to RNAi. Curr. Biol. **12:** 1317–1319.

Sternberg, P. W., 2005 Vulval development (June 25, 2005), *WormBook*, ed. The C. elegans Research Community, WormBook, doi/10.1895/wormbook.1.6.1, http://www.wormbook.org.

Sulston, J. E., and J. Hodgkin, 1988 Methods, in *The Nematode Caenorhabditis elegans*. Cold Spring Harbor Laboratory Press, Cold Spring Harbor, NY.

Thoemke, K., W. Yi, J. M. Ross, S. Kim, V. Reinke *et al.*, 2005 Genome-wide analysis of sex-enriched gene expression during C. elegans larval development. Dev. Biol. **284:** 500–508.

Tilmann, C., and J. Kimble, 2005 Cyclin D regulation of a sexually dimorphic asymmetric cell division. Dev. Cell **9:** 489–499.

Tio, M., G. Udolph, X. Yang and W. Chia, 2001 cdc2 links the Drosophila cell cycle and asymmetric division machineries. Nature **409:** 1063–1067.

Tsou, M. F., A. Hayashi and L. S. Rose, 2003 LET-99 opposes Galpha/GPR signaling to generate asymmetry for spindle positioning in response to PAR and MES-1/SRC-1 signaling. Development **130:** 5717–5730.

Uhlenhaut, N. H., S. Jakob, K. Anlag, T. Eisenberger, R. Sekido *et al.*, 2009 Somatic sex reprogramming of adult ovaries to testes by FOXL2 ablation. Cell **139:** 1130–1142.

Wu, M., and M. A. Herman, 2006 A novel noncanonical Wnt pathway is involved in the regulation of the asymmetric B cell division in C. elegans. Dev. Biol. **293:** 316–329.

Wu, M., and M. A. Herman, 2007 Asymmetric localizations of LIN-17/Fz and MIG-5/Dsh are involved in the asymmetric B cell division in C. elegans. Dev. Biol. **303:** 650–662.

Yu, H., A. Seah, M. A. Herman, E. L. Ferguson, H. R. Horvitz *et al.*, 2009 Wnt and EGF pathways act together to induce C. elegans male hook development. Dev. Biol. **327:** 419–432.

Communicating editor: B. J. Meyer

GENETICS

Supporting Information
http://www.genetics.org/cgi/content/full/genetics.109.116038/DC1

Functional Genomic Identification of Genes Required for Male Gonadal Differentiation in *Caenorhabditis elegans*

Andrea K. Kalis, Mary B. Kroetz, Kathleen M. Larson and David Zarkower

DOI: 10.1534/genetics.109.116038

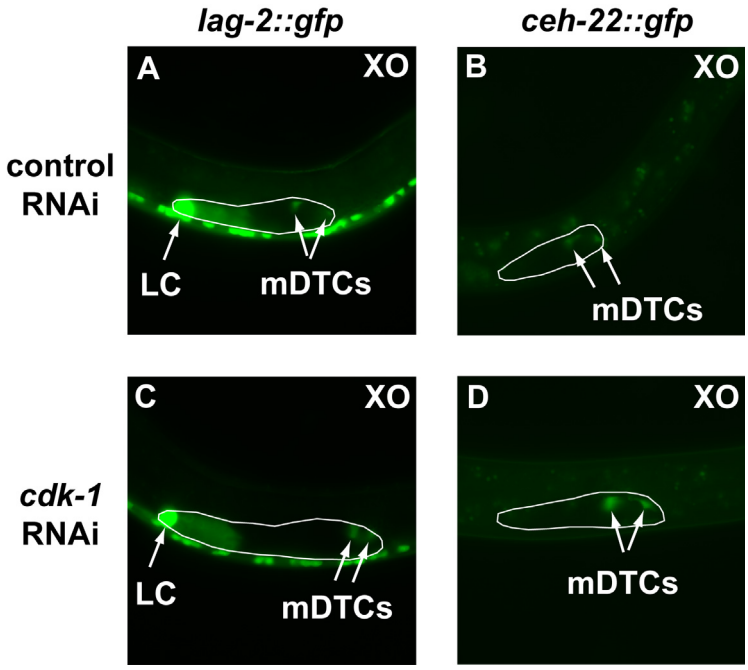

FIGURE S1.—Early gonadal development in *cdk-1(RNAi)* appears normal. (A) *lag-2::GFP* expression in distal tip cells ("mDTCs") and linker cell ("LC") of wild type male (100% n=20). (B) *ceh-22::GFP* expression in distal tip cells of wild type male (100% n=21). (C) Normal number and position of *lag-2::GFP* expressing cells in *cdk-1(RNAi)* male (100% n=21). (D) Nearly normal number and position of *ceh-22::GFP* expressing cells in *cdk-1(RNAi)* animal (90% n=20).

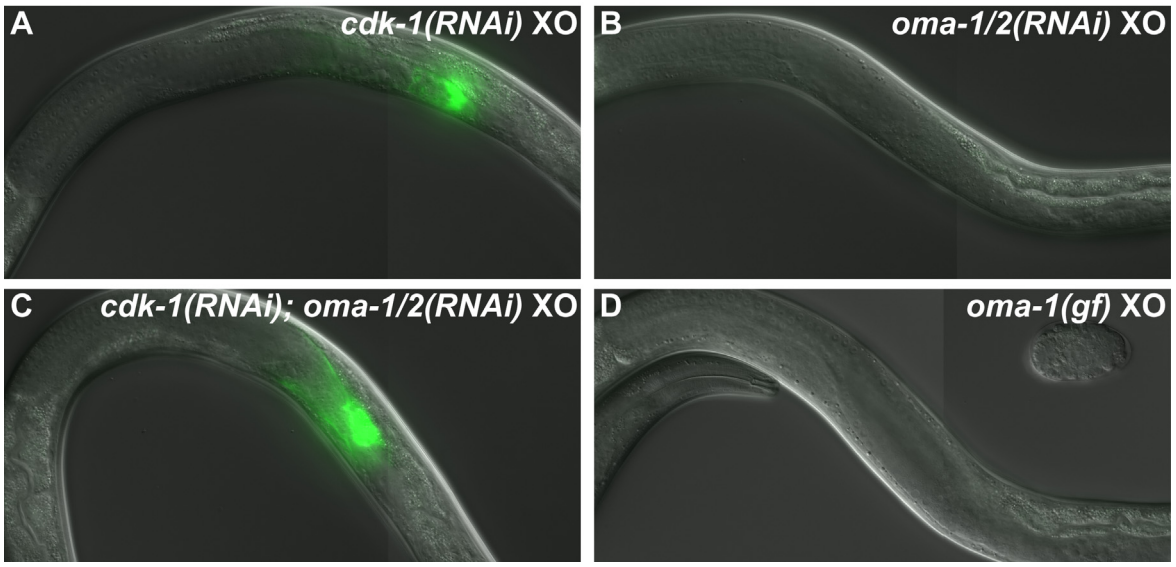

FIGURE S2.—*oma-1/2* destruction is not required for male gonadal cell fate determination. All animals carry the *fkh-6::GFP* marker. (A) *cdk-1(RNAi)* adult males inappropriately express the hermaphrodite-specific spermatheca marker *fkh-6::GFP* in the gonad, indicating feminization of gonadal cells (69% n=16). (B) *oma-1/2(RNAi)* does not cause ectopic *fkh-6::GFP* expression (5% n=22). (C) Feminization of *cdk-1(RNAi)* and *oma-1/2(RNAi)* triple RNAi males is similar to that of *cdk-1(RNAi)* single RNAi (40% n=10). (D) Gonads of *oma-1(zu405)* gain-of-function mutant males are not feminized based on *fkh-6::GFP* expression (3% n=36).

TABLE S1

Genes required for normal gonad marker expression

Sequence Name	Locus	Description	abnormal *fkh-6::GFP* in herm.	n	presence of *fkh-6::GFP* in males	n	abnormal *K09C8.2::GFP* in males	n	gonad defects
control RNAi			0%	86	4%	91	1%	89	-
B0280.1		Protein geranylgeranyltransferase type II, beta subunit	100%	52	0%	22	43%	23	+
B0412.4	rps-29	40S ribosomal protein S29	78%	74	0%	28	71%	21	+
B0464.7	baf-1	DNA-bridging protein BAF	73%	56	0%	22	29%	21	+
B0564.1	tin-9.2	Putative Rrp41 subunit of the exosomal 3'-5' exoribonuclease complex	84%	58	0%	15	57%	21	+
C01G8.9a	let-526	SWI-SNF chromatin-remodeling complex protein	99%	74	0%	25	100%	24	+
C01H6.2		Ankyrin repeat	100%	52	3%	29	71%	28	+
C07A9.3	tlk-1	Tousled-like protein kinase	100%	66	0%	32	48%	33	+
C07G2.3	cct-5	Chaperonin complex component, TCP-1 epsilon subunit	100%	68	0%	28	92%	24	+
C12C8.3	lin-41	Predicted E3 ubiquitin ligase	4%	46	0%	18	14%	21	+
C16A3.3		rRNA processing protein Rrp5	100%	66	0%	23	91%	32	+
C17H12.1	dyci-1	Cytoplasmic dynein intermediate chain	71%	56	0%	27	5%	21	+
C23G10.8			100%	64	0%	26	69%	29	+
C24H11.7	gbf-1	Pattern-formation protein/guanine nucleotide exchange factor	99%	70	0%	25	83%	12	+
C25A1.6		H/ACA snoRNP complex, subunit NOP10	100%	82	0%	35	22%	32	+
C28C12.8	hlh-12		75%	52	0%	23	37%	27	+
C37C3.6	ppn-1	Serine proteinase inhibitor (KU family) with thrombospondin repeats	100%	52	0%	22	63%	24	+
C38C3.5		Actin depolymerizing factor	100%	58	0%	13	83%	23	+
C39E9.14	dli-1	Dynein light intermediate chain	67%	54	0%	22	5%	22	+

C42C1.5			31%	62	0%	25	6%	16	+
C42D4.8	rpc-1	RNA polymerase III, large subunit	100%	58	3%	32	55%	29	+
C48E7.2		RNA polymerase III (C) subunit	77%	78	0%	36	55%	38	+
C53A5.3	had-1	Histone deacetylase complex, catalytic component RPD3	100%	58	0%	20	91%	22	+
D1014.3	snap-1	SNAP (Soluble NSF Attachment Protein) homolog	70%	60	0%	21	7%	60	+
E04A4.4	hoe-1	Predicted metal-dependent hydrolase	84%	64	0%	12	14%	14	+
F09F7.3		RNA polymerase III, second largest subunit	100%	64	0%	23	90%	31	+
F10B5.6	emb-27	APC subunit	100%	62	0%	24	52%	33	+
F11A10.8	cpsf-4	Polyadenylation factor I complex, subunit, Yth1 (CPSF subunit)	55%	58	0%	27	28%	18	+
F19B6.1		Armadillo/beta-Catenin/plakoglobin	41%	56	0%	21	8%	26	+
F27C1.6			15%	68	0%	30	65%	37	+
F28B3.7	him-1		91%	66	0%	27	36%	39	+
F29G9.4a	fos-1	Transcriptional activator FOSB/c-Fos and related bZIP transcription factors	100%	60	0%	17	33%	27	+
F30A10.9		Predicted nucleic-acid-binding protein, contains PIN domain	15%	54	3%	36	11%	36	+
F32A7.6[a]	aex-5	Subtilisin-like proprotein convertase	100%	56	0%	26	100%	27	+
F34D10.2		CDC45-like protein	94%	62	0%	15	15%	34	+
F37C12.13	exos-9	Exosomal 3'-5' exoribonuclease complex, subunit Rrp45	81%	68	3%	31	27%	33	+
F40F12.7		CREB binding protein/P300 and related TAZ Zn-finger proteins	100%	48	0%	27	95%	21	+
F43G9.10		Microfibrillar-associated protein MFAP1	78%	72	0%	35	12%	26	+
F52D10.3	ftt-2	Multifunctional chaperone (14-3-3 family)	5%	94	2%	49	3%	38	+
F54A3.3		Chaperonin complex component, TCP-1 gamma subunit	91%	70	4%	27	100%	35	+
F54C8.2	cpar-1	Histones H3 and H4	18%	74	0%	31	9%	35	+

F54C9.9		Ribosomal protein	56%	68	0%	34	16%	37	+
F54D1.6		Mucin/alpha-tectorin	100%	56	0%	29	11%	19	+
F54H5.4	mua-1	Zn-finger, predicted transcription factor	19%	42	0%	26	15%	33	+
F55A12.8		Predicted P-loop ATPase fused to an acetyltransferase	75%	64	0%	25	92%	37	+
F55F8.3		WD40-repeat-containing subunit of the 18S rRNA processing complex	97%	74	0%	39	86%	39	+
F56A8.6	cpf-2	mRNA cleavage and polyadenylation factor I complex, subunit RNA15	96%	68	0%	27	83%	35	+
F56F10.4		SNARE-interacting protein	35%	60	0%	24	7%	30	-
F58A4.9		DNA-directed RNA polymerase, subunit L	4%	84	0%	28	23%	39	+
H06H21.3		Translation initiation factor 1A (eIF-1A)	77%	44	0%	19	11%	18	+
K01C8.6		Mitochondrial ribosomal protein L10	0%	60	0%	31	0%	11	+
K04D7.1	rack-1	G protein beta subunit-like protein	72%	54	0%	26	4%	26	+
K08F11.4	yrs-1	Tyrosinyl tRNA synthetase predicted to be mitochondrial	100%	70	0%	15	85%	13	+
K09A9.1	nipi-3		100%	56	0%	18	100%	21	+
K12H4.3		RNA-binding protein required for biogenesis of the ribosomal 60S subunit	93%	70	0%	31	52%	33	+
M04B2.1	mep-1		14%	50	0%	26	5%	20	+
R06A10.2	gsa-1	G protein subunit G alphas	96%	54	0%	32	14%	37	+
R06C7.8	bub-1	Mitotic checkpoint serine/threonine protein kinase	100%	74	0%	32	17%	23	+
R10E4.4	mcm-5	DNA replication licensing factor, MCM5 component	97%	66	0%	22	32%	28	+
R166.4	pro-1	WD40 repeat protein	92%	66	0%	34	31%	36	+
T05C12.7	cct-1	Chaperonin complex component, TCP-1 alpha subunit	100%	46	0%	7	92%	13	+
T13F2.7	sna-2	snRNP-binding protein	33%	54	0%	16	7%	29	+
T23D8.3			68%	60	0%	32	18%	38	+

Y22D7AL.5	hsp-60	Mitochondrial chaperonin	96%	54	0%	26	45%	22	+
Y38F1A.5	cyd-1	G1/S-specific cyclin D	98%	50	0%	46	45%	29	+
Y39G10AR.12	tpxl-1		90%	62	0%	32	6%	32	+
Y39G10AR.14	mcm-4	DNA replication licensing factor, MCM4 component	100%	72	2%	41	9%	34	+
Y45F10D.7		WD40 repeat-containing protein	59%	46	0%	19	14%	22	+
Y47D3A.26	smc-3	Structural maintenance of chromosome protein 3 (sister chromatid cohesion complex Cohesin, subunit SMC3)	100%	54	0%	18	41%	27	+
Y47G6A.5			6%	80	0%	34	13%	31	-
Y48B6A.3	xrn-2	5'-3' exonuclease HKE1/RAT1	32%	76	0%	38	100%	46	+
Y48G1A.4		Nucleolar protein involved in 40S ribosome biogenesis	32%	66	3%	31	5%	37	+
Y51H4A.15			8%	52	0%	18	5%	20	+
Y54E10A.10		Protein required for biogenesis of the ribosomal 60S subunit	73%	48	0%	24	19%	26	+
Y54E10BR.5		Signal peptidase I	100%	44	0%	21	19%	21	+
Y71G12B.11		Talin	100%	68	0%	34	15%	33	+
Y92C3B.2	uaf-1	Splicing factor U2AF, large subunit (RRM superfamily)	100%	56	0%	26	57%	21	+
ZC123.3		Homeobox protein	100%	78	0%	39	100%	36	+
ZC434.4		rRNA processing protein RRP7	65%	52	0%	24	17%	24	+
ZK1127.1[a]	nos-2	DNA topoisomerase	100%	68	4%	27	31%	29	+
ZK632.1	mcm-6	DNA replication licensing factor, MCM6 component	99%	74	0%	30	12%	33	+
ZK899.2			0%	40	0%	28	7%	27	+
C14B9.4	plk-1	Polo-like serine/threonine protein kinase	21%	78	0%	39	3%	38	+
C25A11.4	ajm-1	Apical junction molecule, coiled-coil motif	50%	60	0%	17	0%	12	+
E04A4.7	cyc-2.1	Cytochrome c	100%	50	0%	18	0%	9	+

F01F1.7		U5 snRNP-like RNA helicase subunit	92%	48	0%	29	0%	28	+
F28C6.3	cpf-1	mRNA cleavage stimulating factor complex; subunit 1	58%	66	0%	28	3%	33	-
F28D1.1		WD40-repeat-containing subunit of the 18S rRNA processing complex	41%	56	0%	20	0%	19	+
F33H2.5		DNA polymerase epsilon, catalytic subunit A	97%	66	4%	28	0%	33	+
F47F6.1	lin-42	PAS domain, Circadian clock protein period	7%	82	3%	33	0%	6	-
F49C12.8	rpn-7	26S proteasome regulatory complex, subunit RPN7/PSMD6	54%	26	0%	15	0%	8	+
F57B9.5	byn-1	Cell adhesion complex protein bystin	85%	66	3%	29	3%	34	+
F58A4.4[a]	pri-1	Eukaryotic-type DNA primase, catalytic subunit	98%	80	0%	33	4%	26	+
F59D12.4	gpn-1	Glypican, a heparan sulfate proteoglycan	33%	64	4%	23	4%	23	-
H06I04.3		Putative SAM-dependent rRNA methyltransferase SPB1	24%	62	0%	30	3%	30	+
K08A8.2	sox-2	HMG-box transcription factor	93%	60	0%	20	0%	20	+
K09E3.1[a]	kbp-3	Kinetochore binding protein	80%	46	3%	31	0%	16	+
R02F2.7			22%	54	0%	23	3%	30	+
R12B2.4	him-10		60%	62	3%	34	0%	24	+
R53.3	egl-43	Zinc finger	100%	60	0%	35	0%	35	+
T12F5.4	lin-59	Putative transcription factor ASH1/LIN-59	46%	76	3%	31	0%	35	-
T20B12.3		Predicted nucleolar protein involved in ribosome biogenesis	48%	46	0%	19	0%	27	+
W07E6.4	prp-21	Splicing factor	25%	72	3%	29	4%	25	+
Y41E3.11		Scaffold/matrix specific factor hnRNP-U/SAF-A, contains SPRY domain	6%	64	0%	22	0%	24	-
Y45F10D.9	sas-6	Coiled-coil region, novel PISA motif	25%	48	3%	30	0%	26	+
Y53F4B.13		FtsJ-like RNA methyltransferase	95%	60	0%	18	0%	29	+

Y55B1AL.3		DNA polymerase theta/eta, DEAD-box superfamily	71%	72	0%	29	0%	30	+
Y55B1BM.1	stim-1	Cell surface glycoprotein STIM, contains SAM domain	100%	50	0%	27	0%	25	+
Y75B8A.7		U3 small nucleolar ribonucleoprotein (snoRNP) subunit - Mpp10p	16%	70	4%	27	3%	32	-
ZC477.9	deb-1	Alpha-catenin	100%	60	0%	27	0%	25	+
ZK1151.1	vab-10	Dystonin, GAS (Growth-arrest-specific protein)	21%	48	4%	26	0%	37	+
ZK1236.3	sor-1		24%	68	3%	30	0%	38	+
ZK512.2		ATP-dependent RNA helicase	64%	50	0%	21	0%	22	+
ZK520.4	cul-2	E3 ubiquitin ligase, Cullin 2 component	11%	112	0%	41	2%	45	+
ZK686.2		DEAD-box ATP-dependent RNA helicase	82%	68	0%	30	0%	28	+
C15H9.6[a]	hsp-3	Heat shock response 70 protein	0%	50	0%	21	20%	10	+
C27B7.8	rap-1	Ras-related GTPase	0%	56	0%	22	17%	30	+
C43H6.4			0%	40	0%	17	17%	30	+
F13A2.3			0%	60	0%	19	13%	31	-
F15G9.4	him-4	Immunoglobin and related proteins (hemicentin)	2%	96	0%	44	84%	37	+
F30A10.10		Ubiquitin carboxyl-terminal hydrolase	0%	68	0%	32	72%	36	-
F30H5.1	unc-45	Myosin assembly protein/sexual cycle protein and related proteins	0%	82	0%	44	28%	40	+
F36A2.9		Phospholipase	0%	78	0%	23	57%	42	-
F37C12.11	rps-21	40S ribosomal protein S21	2%	76	0%	45	16%	43	+
F55C7.7	unc-73	Guanine nucleotide exchange factor for Rho and Rac GTPases	0%	66	3%	32	7%	27	+
K02B12.1	ceh-6	Transcription factor OCT-1, contains POU and HOX domain	0%	56	0%	18	70%	10	+
K09C8.2			0%	52	0%	23	100%	20	+
R01H10.1	div-1	DNA polymerase alpha-primase complex,	0%	104	2%	46	71%	51	-

		polymerase-associated subunit B							
T01H8.1	rskn-1	Ribosomal protein S6 kinase	0%	72	0%	22	60%	40	-
T07C4.4	spp-1	Predicted transmembrane protein	0%	54	0%	24	9%	22	+
T11F9.4	aat-4	Amino acid transporters	3%	62	0%	24	12%	34	+
T14G10.2	pxf-1	cAMP-regulated guanine nucleotide exchange factor	0%	90	0%	39	41%	46	+
T28B4.4			0%	66	0%	43	9%	35	-
T28F3.3	hke-4.1	Putative zinc transporter	0%	46	0%	22	7%	15	+
W03F8.4		Cell growth regulatory protein CGR11	0%	52	0%	26	11%	27	+
Y39G8B.3	sre-48	Sre G protein-coupled chemoreceptor	0%	66	0%	38	11%	36	-
Y41D4A.5			0%	46	0%	26	12%	26	+
ZK381.5	prkl-1		0%	82	0%	41	4%	52	+
B0207.4	air-2	Serine/threonine protein kinase	87%	60	13%	30	24%	25	+
B0286.5	fkh-6	Forkhead transcription factor	100%	66	30%	57	64%	44	+
C04H5.6	mog-4	mRNA splicing factor ATP-dependent RNA helicase	91%	58	13%	23	0%	24	+
C08C3.1	egl-5	Transcription factor zerknullt and related HOX domain proteins	0%	64	100%	31	30%	33	+
C18D11.4	rps-8	RRM domain	93%	70	6%	31	6%	33	+
C25D7.6	mcm-3	DNA replication licensing factor, MCM3 component	100%	50	13%	24	29%	38	+
C27A2.3	ify-1	Predicted securin	38%	52	12%	26	48%	33	+
C29E4.2	kle-2		100%	70	6%	34	47%	36	+
C30B5.4		RNA binding protein	71%	48	17%	30	53%	36	+
C36E8.5[a]	tbb-2	Beta tubulin	97%	66	43%	21	57%	23	+
C38C10.4[a]	gpr-2	GPR (G Protein Regulator)/GoLoco motif	96%	46	17%	41	21%	38	+
C47B2.3[a]	tba-2	Alpha tubulin	100%	50	60%	35	96%	23	+
C47E8.7	unc-112	Mitogen inducible gene product (contains ERM and PH domains)	100%	60	4%	28	38%	21	+
C50F2.3		mRNA splicing factor	100%	40	10%	20	71%	21	+
C52E4.6	cyl-1	Cyclin L	100%	38	19%	21	100%	31	+

C54D1.5	lam-2	Laminin gamma subunit	100%	50	15%	27	100%	24	+
C54D1.6	bar-1	Armadillo/beta-Catenin/plakoglobin	9%	54	5%	20	8%	24	+
C56C10.8	icd-1	RNA polymerase II	94%	70	53%	30	19%	32	+
F10E9.4			100%	68	40%	30	97%	30	+
F12F6.7		DNA polymerase delta, regulatory subunit 55	88%	84	9%	47	25%	32	+
F16B4.8	cdc-25.2	M-phase inducer phosphatase	100%	54	50%	26	64%	28	+
F17E9.12	his-31	Histone H4	0%	92	6%	32	17%	35	-
F18A1.5	rpa-1	Replication protein	100%	62	19%	21	100%	22	+
F19F10.9		U4/U6.U5 snRNP associated protein	100%	60	38%	24	54%	26	+
F20D6.11		Monodehydroascorbate/ferredoxin reductase	0%	56	5%	22	11%	28	+
F25H8.3	gon-1	MPT (metalloprotease with thrombospondin type 1 repeats)	100%	54	11%	38	96%	27	+
F32H2.3			100%	48	17%	24	79%	34	+
F35B12.5	sas-5	Coiled-coil protein	100%	56	23%	35	33%	27	+
F38A6.1	pha-4	Forkhead/HNF-3-related transcription factor	100%	58	8%	26	27%	26	+
F38H4.9	let-92	Serine/threonine protein phosphatase 2A, catalytic subunit	94%	54	5%	20	70%	30	+
F40F11.2			75%	60	13%	23	10%	39	+
F55F10.1		AAA ATPase	45%	44	8%	25	5%	21	+
F56A3.4	spd-2		94%	72	36%	28	40%	43	+
F58A4.8	tbg-1	Gamma tubulin	17%	82	7%	41	5%	38	+
F59A2.1	npp-9	Ran-binding protein RANBP1 and related RanBD domain proteins	77%	64	7%	30	52%	27	+
K06A5.4	knl-2		100%	62	13%	30	100%	21	+
K07A1.2	dut-1	dUTPase	92%	48	24%	25	42%	26	+
K08C7.3	epi-1	Extracellular matrix glycoprotein Laminin subunits alpha and gamma	100%	56	7%	30	100%	20	+

K12C11.2	smo-1	Ubiquitin-like proteins	77%	52	54%	26	65%	34	+
M03D4.1	zen-4	Kinesin-like protein	45%	94	23%	43	32%	44	+
T05G5.3	cdk-1	Protein kinase PCTAIRE and related kinases	55%	82	88%	52	82%	45	+
T06E6.2	cyb-3	Cyclin B and related kinase-activating proteins	100%	60	22%	23	76%	25	+
T07A9.9		GTP-binding protein	100%	62	15%	20	27%	22	+
T11G6.8		Predicted RNA-binding protein (RRM superfamily)	100%	52	18%	22	57%	23	+
T13H5.4		Splicing factor	100%	70	38%	21	18%	22	+
T20B12.8	hmg-4	Nucleosome-binding factor SPN, POB3 subunit	16%	88	5%	43	24%	50	+
T22D1.10	ruvb-2	DNA helicase TIP49, TBP-interacting protein	92%	60	10%	29	8%	26	+
T23D8.9	sys-1	Novel protein that contains three divergent armadillo repeats	100%	58	50%	26	39%	28	+
T24B8.6	hlh-3	Transcription factor HAND2/Transcription factor	0%	78	7%	42	20%	46	+
T25G3.3		NMD protein affecting ribosome stability and mRNA decay	97%	74	9%	32	51%	35	+
W01D2.2	nhr-61	Nuclear hormone receptor	86%	76	21%	33	33%	24	+
W02D9.1	pri-2	Eukaryotic-type DNA primase, large subunit	100%	76	9%	22	52%	25	+
W03C9.4	lin-29	Zinc finger transcription factor	0%	62	7%	29	23%	26	+
W06F12.1	lit-1	Nemo-like MAPK-related serine/threonine protein kinase	79%	66	81%	32	71%	34	+
W07B3.2	gei-4		14%	84	15%	41	73%	40	+
W08D2.7	mtr-4	Nuclear exosomal RNA helicase MTR4, DEAD-box superfamily	98%	48	17%	29	60%	20	+
W10C8.2	pop-1	Transcription factor TCF-4	100%	62	77%	22	72%	25	+
Y110A7A.1	hcp-6	Uncharacterized conserved protein related	100%	62	9%	23	59%	29	+

		to condensin complex subunit 1							
Y119D3B.22	fbxa-76	F-box A protein	0%	60	4%	25	15%	27	-
Y39A1A.12		Origin recognition complex, subunit 1, and related proteins	100%	52	22%	23	100%	25	+
Y39G10AR.13	icp-1	Inner centromere protein (INCENP), C-terminal domain	81%	58	11%	27	64%	28	+
Y41D4B.5	rps-28	40S ribosomal protein S28	96%	54	15%	20	52%	23	+
Y47G6A.20	rpn-6	26S proteasome regulatory complex, subunit RPN6/PSMD11	100%	58	12%	26	50%	24	+
Y51H4A.3	rho-1	Ras-related small GTPase, Rho type	100%	60	5%	21	32%	22	+
Y65B4BR.5		Transcription factor containing NAC and TS-N domains	100%	64	30%	30	85%	41	+
Y76B12C.7		mRNA cleavage and polyadenylation factor II complex, subunit CFT1 (CPSF subunit)	20%	64	6%	34	0%	27	+
control RNAi			0%	86	4%	91	1%	89	-

Genes are arranged by class (see Results): Class I (grey); Class II (rose); Class III (yellow); Class IV (teal).
[a]RNAi clone may target more than one transcript

TABLE S2

Genes required for normal gonadal development

		hermaphrodite				male			
Sequence Name	Locus	not fully elongated gonad arms	lack of oocytes	fertility[b]	n	not fully elongated gonad	abnormal germline	abnormal seminal vessicle/vas deferens	n
control RNAi		0%	0%	+++	86	0%	0%	0%	47
B0207.4	air-2	0%	0%	NE	60	4%	28%	36%	25
B0280.1		0%	0%	NE	52	6%	88%	65%	17
B0286.5	fkh-6	3%	0%	NE	66	48%	0%	55%	44
B0412.4	rps-29	8%	38%	NE	50	32%	18%	41%	22
B0464.7	baf-1	0%	50%	++	56	9%	9%	23%	22
B0564.1	tin-9.2	0%	0%	DE	58	14%	5%	48%	21
C01G8.9a	let-526	0%	0%	NE	74	86%	0%	86%	21
C01H6.2		0%	53%	NE	30	39%	46%	100%	28
C04H5.6	mog-4	0%	0%	DE +	58	13%	4%	8%	24
C07A9.3	tlk-1	0%	0%	NE	66	15%	0%	15%	33
C07G2.3	cct-5	0%	0%	NE	68	4%	0%	21%	24
C08C3.1	egl-5	0%	0%	+++	64	88%	0%	88%	33
C12C8.3	lin-41	0%	0%	NE	46	0%	0%	0%	21
C14B9.4	plk-1	0%	0%	DE +	78	0%	0%	0%	38
C15H9.6	hsp-3	0%	0%	+++	50	20%	20%	20%	10
C16A3.3		0%	100%	NE	66	9%	0%	47%	32
C17H12.1	dyci-1	0%	0%	DE	56	0%	5%	5%	21
C18D11.4	rps-8	0%	0%	DE +	70	3%	0%	3%	33
C23G10.8		0%	0%	NE	64	3%	0%	3%	29
C24H11.7	gbf-1	2%	54%	NE	56	33%	0%	50%	12
C25A1.6		0%	5%	NE	82	0%	0%	0%	32
C25A11.4	ajm-1	0%	0%	DE	60	0%	0%	0%	12
C25D7.6	mcm-3	0%	0%	NE	50	25%	6%	50%	16
C27A2.3	ify-1	11%	27%	DE	56	35%	0%	35%	37
C27B7.8	rap-1	0%	0%	+++	56	17%	0%	20%	30
C28C12.8	hlh-12	0%	0%	+++	52	37%	4%	37%	27
C29E4.2	kle-2	0%	0%	NE	70	38%	0%	38%	32
C30B5.4		0%	0%	DE	48	3%	3%	10%	31
C36E8.5	tbb-2	67%	74%	DE +	46	47%	20%	47%	15
C37C3.6	ppn-1	100%	100%	NE	52	67%	0%	71%	24
C38C10.4	gpr-2	0%	61%	NE	46	25%	6%	44%	16
C38C3.5		0%	0%	NE	58	100%	0%	100%	23
C39E9.14	dli-1	0%	0%	++	54	0%	0%	0%	22

C42C1.5		0%	0%	DE +	62	0%	0%	6%	16
C42D4.8	rpc-1	0%	52%	NE	58	0%	4%	38%	24
C43H6.4		0%	0%	+++	40	3%	10%	10%	30
C47B2.3	tba-2	100%	100%	NE	50	78%	11%	100%	9
C47E8.7	unc-112	0%	0%	NE	60	24%	0%	24%	21
C48E7.2		0%	0%	NE	78	0%	0%	5%	38
C50F2.3		0%	100%	NE	40	86%	0%	86%	7
C52E4.6	cyl-1	0%	100%	NE	38	30%	22%	100%	27
C53A5.3	had-1	0%	0%	NE	58	35%	0%	35%	26
C54D1.5	lam-2	100%	100%	NE	50	100%	100%	100%	24
C54D1.6	bar-1	0%	0%	++	54	12%	6%	12%	17
C56C10.8	icd-1	0%	0%	NE	70	0%	0%	0%	32
D1014.3	snap-1	0%	0%	DE	60	12%	4%	12%	26
E04A4.4	hoe-1	0%	0%	DE +	64	7%	21%	14%	14
E04A4.7	cyc-2.1	0%	0%	DE	50	0%	0%	0%	9
F01F1.7		0%	0%	DE +	48	0%	0%	0%	28
F09F7.3		0%	88%	NE	64	0%	90%	3%	31
F10B5.6	emb-27	0%	0%	NE	62	0%	0%	0%	33
F10E9.4		0%	100%	NE	68	67%	26%	74%	27
F11A10.8	cpsf-4	0%	0%	DE	58	28%	17%	28%	18
F12F6.7		0%	50%	DE +	84	15%	11%	22%	27
F15G9.4	him-4	0%	0%	++	76	92%	0%	92%	37
F16B4.8	cdc-25.2	0%	0%	DE	54	47%	6%	47%	32
F18A1.5	rpa-1	0%	100%	NE	62	82%	23%	100%	22
F19B6.1		0%	0%	++	56	8%	4%	8%	26
F19F10.9		0%	100%	NE	60	68%	9%	64%	22
F20D6.11		0%	0%	+++	56	13%	13%	19%	32
F25H8.3	gon-1	100%	56%	NE	54	100%	0%	100%	27
F27C1.6		0%	0%	DE +	68	0%	0%	14%	37
F28B3.7	him-1	0%	79%	NE	66	13%	3%	23%	39
F28D1.1		0%	0%	DE +	56	0%	0%	0%	19
F29G9.4a	fos-1	30%	55%	NE	40	4%	96%	4%	27
F30A10.9		0%	30%	DE +	54	6%	3%	6%	32
F30H5.1	unc-45	0%	89%	NE	82	0%	0%	3%	40
F32A7.6[a]	aex-5	0%	0%	++	26	13%	3%	13%	30
F32H2.3		0%	0%	NE	48	59%	5%	65%	37
F33H2.5		0%	0%	NE	66	0%	0%	0%	33
F34D10.2		0%	0%	NE	62	0%	0%	0%	34
F35B12.5	sas-5	0%	100%	+	56	48%	11%	52%	27
F37C12.11	rps-21	2%	2%	NE	76	12%	0%	12%	43

F37C12.13	exos-9	0%	0%	DE +	68	0%	0%	0%	33
F38A6.1	pha-4	100%	100%	NE	58	4%	0%	31%	26
F38H4.9	let-92	24%	24%	NE	54	60%	0%	60%	15
F40F11.2		0%	0%	NE	60	23%	0%	15%	13
F40F12.7		0%	0%	NE	48	81%	5%	81%	21
F43G9.10		0%	0%	NE	72	8%	0%	8%	26
F49C12.8	rpn-7	0%	0%	NE	26	13%	13%	13%	8
F52D10.3	ftt-2	0%	0%	NE	78	0%	0%	0%	38
F54A3.3		0%	100%	NE	60	3%	6%	80%	35
F54C8.2	cpar-1	0%	0%	DE	74	0%	11%	0%	35
F54C9.9		0%	0%	DE +	68	0%	0%	0%	37
F54D1.6		0%	0%	NE	56	0%	16%	10%	19
F54H5.4	mua-1	0%	0%	++	42	12%	12%	15%	33
F55A12.8		0%	25%	NE	64	5%	0%	57%	37
F55C7.7	unc-73	0%	0%	+++	66	63%	0%	55%	27
F55F10.1		0%	0%	DE	44	0%	0%	0%	8
F55F8.3		0%	0%	NE	74	3%	0%	28%	39
F56A3.4	spd-2	1%	0%	NE	72	13%	0%	20%	45
F56A8.6	cpf-2	0%	0%	DE	68	0%	0%	11%	35
F57B9.5	byn-1	0%	0%	DE +	66	0%	0%	0%	34
F58A4.4	pri-1	0%	0%	NE	80	0%	0%	0%	26
F58A4.8	tbg-1	0%	0%	DE +	82	3%	0%	3%	38
F58A4.9		0%	0%	DE +	84	4%	0%	7%	45
F59A2.1	npp-9	0%	72%	DE	64	8%	0%	11%	27
H06H21.3		0%	0%	NE	44	0%	0%	0%	18
H06I04.3		0%	0%	+	64	0%	0%	0%	30
K01C8.6		0%	0%	DE +	60	0%	0%	0%	11
K02B12.1	ceh-6	0%	0%	NE	56	0%	0%	20%	10
K04D7.1	rack-1	0%	0%	NE	54	0%	19%	0%	26
K06A5.4	knl-2	32%	100%	NE	62	100%	0%	0%	19
K07A1.2	dut-1	3%	59%	DE	32	25%	4%	32%	28
K08A8.2	sox-2	0%	0%	NE	60	0%	0%	0%	20
K08C7.3	epi-1	100%	86%	NE	56	100%	0%	100%	20
K08F11.4	yrs-1	0%	0%	NE	70	0%	38%	15%	13
K09A9.1	nipi-3	0%	0%	NE	56	0%	38%	5%	21
K09C8.2		0%	0%	+++	52	15%	10%	15%	20
K09E3.1	kbp-3	0%	0%	+	46	0%	0%	0%	16
K12C11.2	smo-1	0%	0%	NE	52	3%	0%	13%	32
K12H4.3		0%	0%	NE	70	0%	0%	23%	30
M03D4.1	zen-4	43%	97%	NE	68	22%	6%	31%	36
M04B2.1	mep-1	0%	0%	++	50	0%	0%	0%	20

R02F2.7		0%	0%	DE +	54	0%	0%	0%	30
R06A10.2	gsa-1	0%	0%	NE	54	0%	0%	0%	37
R06C7.8	bub-1	0%	0%	NE	74	0%	0%	0%	23
R10E4.4	mcm-5	0%	0%	NE	66	4%	0%	0%	28
R12B2.4	him-10	0%	0%	+	62	0%	0%	0%	24
R166.4	pro-1	0%	9%	NE	66	0%	0%	0%	36
R53.3	egl-43	0%	0%	NE	60	0%	0%	0%	35
T05C12.7	cct-1	0%	100%	NE	46	46%	31%	46%	13
T05G5.3	cdk-1	33%	33%	NE	66	42%	12%	61%	33
T06E6.2	cyb-3	10%	60%	NE	40	72%	0%	84%	25
T07A9.9		0%	100%	NE	62	0%	20%	60%	10
T07C4.4	spp-1	0%	0%	+++	54	9%	9%	9%	22
T11F9.4	aat-4	0%	0%	+++	62	9%	3%	12%	34
T11G6.8		4%	57%	NE	46	31%	0%	56%	16
T13F2.7	sna-2	0%	0%	DE +	54	3%	7%	10%	29
T13H5.4		0%	86%	NE	70	0%	36%	41%	22
T14G10.2	pxf-1	0%	0%	+++	90	30%	0%	55%	44
T20B12.3		0%	0%	+	46	0%	0%	0%	27
T20B12.8	hmg-4	0%	0%	DE ++	88	9%	2%	9%	44
T22D1.10	ruvb-2	0%	40%	DE +	60	0%	0%	0%	26
T23D8.3		0%	48%	DE +	50	3%	0%	3%	38
T23D8.9	sys-1	42%	63%	NE	38	29%	4%	29%	28
T24B8.6	hlh-3	0%	0%	+++	78	17%	0%	14%	46
T25G3.3		0%	0%	+	74	0%	0%	0%	35
T28F3.3	hke-4.1	0%	0%	+++	46	7%	0%	7%	15
W01D2.2	nhr-61	0%	13%	DE +	76	17%	0%	17%	24
W02D9.1	pri-2	0%	95%	NE	76	4%	4%	4%	25
W03C9.4	lin-29	0%	0%	+++	62	15%	0%	15%	20
W03F8.4		0%	0%	+++	52	11%	11%	11%	27
W06F12.1	lit-1	0%	0%	NE	66	0%	0%	3%	34
W07B3.2	gei-4	0%	0%	NE	76	23%	0%	61%	31
W07E6.4	prp-21	0%	0%	DE +	72	0%	0%	0%	25
W08D2.7	mtr-4	0%	100%	NE	48	0%	0%	100%	14
W10C8.2	pop-1	58%	56%	NE	62	64%	8%	64%	25
Y110A7A.1	hcp-6	0%	0%	DE	62	48%	0%	52%	29
Y22D7AL.5	hsp-60	0%	0%	DE +	54	0%	32%	4%	25
Y38F1A.5	cyd-1	22%	0%	NE	50	28%	0%	41%	29
Y39A1A.12		0%	100%	NE	52	100%	0%	100%	17
Y39G10AR.12	tpxl-1	0%	0%	DE +	64	6%	0%	6%	32
Y39G10AR.13	icp-1	0%	35%	DE	46	8%	4%	12%	25
Y39G10AR.14	mcm-4	0%	0%	NE	72	0%	0%	0%	34

Y41D4A.5		0%	0%	+++	46	5%	5%	9%	22
Y41D4B.5	rps-28	0%	100%	NE	54	28%	89%	83%	18
Y45F10D.7		0%	0%	DE +	46	5%	14%	14%	22
Y45F10D.9	sas-6	0%	0%	+	48	0%	0%	0%	26
Y47D3A.26	smc-3	0%	0%	NE	54	33%	0%	33%	24
Y47G6A.20	rpn-6	0%	100%	NE	58	68%	26%	95%	19
Y48B6A.3	xrn-2	0%	91%	NE	76	0%	2%	93%	42
Y48G1A.4		0%	0%	++	66	5%	0%	5%	37
Y51H4A.15		0%	0%	+	52	0%	0%	5%	20
Y51H4A.3	rho-1	0%	50%	NE	60	27%	5%	27%	22
Y53F4B.13		0%	0%	DE +	60	0%	0%	0%	29
Y54E10A.10		0%	50%	DE	40	8%	12%	19%	26
Y54E10BR.5		0%	0%	NE	44	14%	5%	19%	21
Y55B1AL.3		0%	0%	DE +	72	0%	0%	0%	30
Y55B1BM.1	stim-1	0%	0%	NE	50	0%	0%	0%	25
Y57G11C.12	nuo-3	0%	0%	NE	54	0%	0%	0%	19
Y65B4BR.5		0%	0%	NE	64	0%	0%	85%	41
Y71G12B.11		0%	0%	NE	68	35%	0%	32%	34
Y76B12C.7		0%	0%	+++	64	0%	18%	0%	22
Y92C3B.2	uaf-1	0%	100%	NE	56	65%	18%	71%	17
ZC123.3		0%	0%	NE	78	0%	0%	0%	36
ZC434.4		0%	0%	DE +	52	8%	17%	21%	24
ZC477.9	deb-1	0%	0%	NE	60	0%	0%	0%	25
ZK1127.1[a]	nos-2	0%	0%	NE	68	14%	3%	14%	29
ZK1151.1	vab-10	0%	0%	DE +	48	3%	0%	3%	37
ZK1236.3	sor-1	5%	22%	DE +	64	0%	0%	0%	38
ZK381.5	prkl-1	0%	0%	+++	82	7%	0%	4%	45
ZK512.2		0%	0%	+	50	0%	0%	0%	22
ZK520.4	cul-2	0%	0%	DE	112	2%	0%	2%	45
ZK632.1[a]	mcm-6	0%	0%	NE	74	0%	0%	0%	33
ZK686.2		0%	0%	+	68	0%	0%	0%	28
ZK899.2		0%	0%	+++	40	7%	7%	7%	27

[a]RNAi clone may target more than one transcript
[b]The number of F2 progeny. NE=No Eggs, DE=Dead Eggs, +=<~30% of control, ++=~30-90% of control, +++=~control

TABLE S3

Genes whose depletion feminizes male gonads

Sequence Name	Locus	Description	presence of fkh-6::GFP in males	n	presence of lim-7::GFP in males	n	abnormal K09C8.2::GFP in males	n	male gonadal defects
L4440			4%	91	1%	77	1%	89	-
B0207.4	air-2	Serine/threonine protein kinase	13%	30	0%	31	24%	25	+
B0286.5	fkh-6	Forkhead transcription factor	30%	57	10%	21	64%	44	+
C04H5.6	mog-4	mRNA splicing factor ATP-dependent RNA helicase	13%	23	3%	33	0%	24	+
C08C3.1	egl-5	Transcription factor zerknullt and related HOX domain proteins	100%	31	24%	29	30%	33	+
C18D11.4	rps-8	RRM domain	6%	31	0%	24	6%	33	-
C25D7.6	mcm-3	DNA replication licensing factor, MCM3 component	13%	24	21%	24	29%	38	+
C27A2.3	ify-1	Predicted securin	12%	26	5%	20	48%	33	+
C29E4.2	kle-2		6%	34	0%	32	47%	36	+
C30B5.4		RNA binding protein	17%	30	0%	37	53%	36	+
C36E8.5[a]	tbb-2	Beta tubulin	43%	21	6%	36	57%	23	+
C38C10.4[a]	gpr-2	GPR (G Protein Regulator)/GoLoco motif	17%	41	0%	28	21%	38	+
C47B2.3[a]	tba-2	Alpha tubulin	60%	35	3%	37	96%	23	+
C47E8.7	unc-112	Mitogen inducible gene product (contains ERM and PH domains)	4%	28	0%	39	38%	21	+
C50F2.3		mRNA splicing factor	10%	20	0%	50	71%	21	+
C52E4.6	cyl-1	Cyclin L	19%	21	9%	22	100%	31	+
C54D1.5	lam-2	Laminin gamma subunit	15%	27	0%	34	100%	24	+
C54D1.6	bar-1	Armadillo/beta-Catenin/plakoglobin	5%	20	0%	32	8%	24	+
C56C10.8	icd-1	RNA polymerase II	53%	30	5%	37	19%	32	-
F10E9.4			40%	30	0%	40	97%	30	+
F12F6.7		DNA polymerase delta, regulatory subunit 55	9%	47	18%	33	25%	32	+
F16B4.8	cdc-25.2	M-phase inducer phosphatase	50%	26	3%	38	64%	28	+
F17E9.12	his-31	Histone H4	6%	32	0%	32	17%	35	-
F18A1.5	rpa-1	Replication protein	19%	21	11%	37	100%	22	+
F19F10.9		U4/U6.U5 snRNP associated protein	38%	24	0%	41	54%	26	+
F20D6.11[b]		Monodehydroascorbate/ferredoxin reductase	5%	22	3%	39	11%	28	+
F25H8.3	gon-1	MPT (metalloprotease with thrombospondin type 1 repeats)	11%	38	4%	51	96%	27	+

F32H2.3			17%	24	0%	33	79%	34	+
F35B12.5	sas-5	Coiled-coil protein	23%	35	0%	34	33%	27	+
F38A6.1	pha-4	Forkhead/HNF-3-related transcription factor	8%	26	0%	30	27%	26	+
F38H4.9	let-92	Serine/threonine protein phosphatase 2A, catalytic subunit	5%	20	4%	27	70%	30	+
F40F11.2			13%	23	7%	43	10%	39	-
F55F10.1		AAA ATPase	8%	25	0%	32	5%	21	-
F56A3.4	spd-2		36%	28	3%	39	40%	43	+
F58A4.8	tbg-1	Gamma tubulin	7%	41	0%	21	5%	38	-
F59A2.1	npp-9	Ran-binding protein RANBP1 and related RanBD domain proteins	7%	30	6%	35	52%	27	+
K06A5.4	knl-2		13%	30	0%	32	100%	21	+
K07A1.2	dut-1	dUTPase	24%	25	3%	30	42%	26	+
K08C7.3	epi-1	Extracellular matrix glycoprotein Laminin subunits alpha and gamma	7%	30	3%	34	100%	20	+
K12C11.2	smo-1	Ubiquitin-like proteins	54%	26	3%	38	65%	34	+
M03D4.1	zen-4	Kinesin-like protein	23%	43	0%	33	32%	44	+
T05G5.3	cdk-1	Protein kinase PCTAIRE and related kinases	88%	52	11%	37	82%	45	+
T06E6.2	cyb-3	Cyclin B and related kinase-activating proteins	22%	23	0%	35	76%	25	+
T07A9.9		GTP-binding protein	15%	20	0%	34	27%	22	+
T11G6.8		Predicted RNA-binding protein (RRM superfamily)	18%	22	0%	33	57%	23	+
T13H5.4		Splicing factor	38%	21	5%	37	18%	22	+
T20B12.8	hmg-4	Nucleosome-binding factor SPN, POB3 subunit	5%	43	11%	37	24%	50	+
T22D1.10	ruvb-2	DNA helicase TIP49, TBP-interacting protein	10%	29	0%	36	8%	26	-
T23D8.9	sys-1	Novel beta-catenin	50%	26	14%	42	39%	28	+
T24B8.6[b]	hlh-3	Transcription factor HAND2/Transcription factor	7%	42	0%	35	20%	46	+
T25G3.3		NMD protein affecting ribosome stability and mRNA decay	9%	32	0%	35	51%	35	-
W01D2.2	nhr-61	Nuclear hormone receptor	21%	33	3%	36	33%	24	+
W02D9.1	pri-2	Eukaryotic-type DNA primase, large subunit	9%	22	5%	37	52%	25	-
W03C9.4[b]	lin-29	Zinc finger transcription factor	7%	29	4%	27	23%	26	+
W06F12.1	lit-1	Nemo-like MAPK-related serine/threonine protein kinase	81%	32	11%	37	71%	34	-

W07B3.2	gei-4		15%	41	0%	39	73%	40	+
W08D2.7	mtr-4	Nuclear exosomal RNA helicase MTR4, DEAD-box superfamily	17%	29	0%	37	60%	20	+
W10C8.2	pop-1	Transcription factor TCF-4	77%	22	0%	34	72%	25	+
Y110A7A.1	hcp-6	Uncharacterized conserved protein related to condensin complex subunit 1	9%	23	6%	35	59%	29	+
Y119D3B.22	fbxa-76	F-box A protein	4%	25	0%	38	15%	27	-
Y39A1A.12		Origin recognition complex, subunit 1, and related proteins	22%	23	8%	36	100%	25	+
Y39G10AR.13	icp-1	Inner centromere protein (INCENP), C-terminal domain	11%	27	2%	41	64%	28	+
Y41D4B.5	rps-28	40S ribosomal protein S28	15%	20	6%	32	52%	23	+
Y47G6A.20	rpn-6	26S proteasome regulatory complex, subunit RPN6/PSMD11	12%	26	3%	32	50%	24	+
Y51H4A.3	rho-1	Ras-related small GTPase, Rho type	5%	21	0%	37	32%	22	+
Y65B4BR.5		Transcription factor containing NAC and TS-N domains	30%	30	0%	31	85%	41	+
Y76B12C.7[b]		mRNA cleavage and polyadenylation factor II complex, subunit CFT1 (CPSF subunit)	6%	34	0%	34	0%	27	+
ZK1151.1	vab-10	Dystonin, GAS (Growth-arrest-specific protein)	4%	26	5%	38	0%	37	-

[a]RNAi clone may target more than one transcript
[b]Male specific gonadal defects